Role of Cable Forces in the Model Updating of Cable-Stayed Bridges

The role of cable forces in the model updating of cable-stayed bridges

Angelo Aloisio[1], Dag Pasquale Pasca[2], Marco Martino Rosso[3], and Bruno Briseghella[4]

[1]Department of Civil, Construction-Architectural and Environmental Engineering, University of L'Aquila, via Giovanni Gronchi n.18, L'Aquila, 67100, Italy.

[2]Norsk Treteknisk Institutt (Norwegian Institute of Wood Technology), Børrestuveien 3, 0373, Oslo, Norway.

[3]Department of Structural, Geotechnical and Building Engineering, Politecnico di Torino, Corso Duca degli Abruzzi, 24, Turin, 10128, Italy. (Corresponding author) Email: marco.rosso@polito.it

[4]College of Civil Engineering, Fuzhou University, No. 2 Xue Yuan Road, 350108 Fuzhou, Fujian Province, PR China

ABSTRACT

This paper presents and discusses the feasibility of complete model updating of cable-stayed bridges using experimental estimates of the cable forces and modal parameters. The procedure is applied to the model updating of a curved cable-stayed bridge in Venice (Italy). Conventional optimization problems of mass and stiffness using ambient vibration data are prone to ill-posedness and ill-conditioning. Generally, the scholar must assume one of the two to achieve a trustworthy optimization. This paper demonstrates that it is possible to assess a large set of parameters affecting the mass and stiffness of a cable-stayed bridge following a step-wise procedure based on ambient vibration tests. Preliminary variance-based sensitivity analysis supports the reduction in the number of parameters to be calibrated. Then, the selected parameters are tuned using a meta-heuristic optimization algorithm. In the considered case study, the sensitivity analyses highlight the significance of the following: the concrete mass, the vertical stiffness of the bearings, and the

concrete Young's modulus of the deck and the tower. However, optimizing all the unknowns using a single objective function does not lead to optima within the search domain. Therefore, the authors show that a three-step optimization is required in the considered case study to achieve convergence within the parameters space. As a result, all the twelve modes of the calibrated model perfectly match the experimental ones, with the Modal Assurance Criterion (MAC) higher than 0.9. In addition, the cable forces of the calibrated model present a good match with the experimental ones, with an average percentage error equal to 11%.

INTRODUCTION

Finite element (FE) updating of large-scale structures is a challenging task using traditional optimization methods (Friswell and Mottershead 1995). Classical parametric FE updating is based on comparing experimental and simulated modal parameters. The main drawback of parametric optimization using the modal parameters extracted from ambient vibration data is indeterminacy when assessing the stiffness, and mass matrix simultaneously (Simoen et al. 2015). Operational modal analysis (OMA) returns unscaled mode shapes, which cannot be used to simultaneously estimate the elastic and inertial features of a structural model (Rainieri and Fabbrocino 2014). The optimization problem would be ill-posed and requires the selection of either the inertia or stiffness as unknown parameters.

However, there can be exceptions, and in some instances, ambient vibration data could be used to update the inertial and structural stiffness features reliably. It could be the case of cable-stayed bridges (Zárate and Caicedo 2008), where an experimental estimate of the cables' natural frequencies and the deck's modal parameters can be obtained. The natural frequencies of the cables can return an indirect assessment of the cable forces using suitable mechanical models of the cable dynamics (Irvine 1981; Zhao et al. 2020).

Mechanical intuition suggests that the cable forces, if the cable almost behaves like a linear taut string (Graff 2012), largely depend on the mass of the suspended structure. At the same time, the modal parameters are affected by both the mass and the structural stiffness. Therefore, a step-wise model updating could be carried out in cable-stayed bridges using the cable forces and the modal parameters, respectively.

Optimizing parameters affecting both the inertial and stiffness features represents a problem analogous to estimating scaling factors of mode shapes in operational modal analysis. Since the forces in OMA are unknown, the mode shapes cannot be mass normalized, and only the un-scaled mode shapes can be determined for each mode (Parloo et al. 2001; Parloo et al. 2002; Parloo et al. 2003; Parloo et al. 2005; Brincker and Andersen 2003). Therefore, scaling the mode shapes to the mass matrix would allow a well-posed optimization problem when estimating the mass and stiffness matrices from OMA. Since the majority of existing structures are not cable-stayed, several scholars devised alternative and more general strategies to get information about the structural mass based on modifications of the structure by changing the stiffness and the mass during OMA (Bernal and Gunes 2002; Bernal 2004; Brandt et al. 2019). The most known scaling techniques is the mass-change method (Parloo et al. 2001; Parloo et al. 2002; Brincker and Andersen 2003; Lopez Aenlle et al. 2005), although there are another approaches based on exogenous inputs (López Aenlle et al. 2007; Parloo et al. 2005) or moving loads (Tian et al. 2019; Tian et al. 2021; Sheibani and Ghorbani-Tanha 2021). For instance, the mass-change method involves attaching masses to the points of the structure where the mode shapes of the unmodified structure are known. The mass-change method has also been used in FE-model updating, where the modal parameters of the modified structure are used as additional information to calibrate the mass, and the stiffness matrices of the system (Shahverdi et al. 2005). This approach has been validated by experimental testing of lab-tested structure scale models (Lopez Aenlle et al. 2005), bridges (Parloo et al. 2005), buildings (Brincker et al. 2004), and mechanical systems (Parloo et al. 2001). In cable-stayed bridges, the additional information required for a complete FE model updating is provided by the cable forces, determined from their vibration response by assuming a specific dynamic response model. Achieving an almost complete model updating is particularly relevant for structural health monitoring (Arangio and Bontempi 2015; Li and Ou 2016) and in particular for the identification of damage (Talebinejad et al. 2011; Babajanian Bisheh et al. 2019; Ni et al. 2008).

The cable-stayed bridge selected for the current analysis is the bridge of Porto Marghera in Venice (Italy) (Briseghella et al. 2021; Gentile and Siviero 2007; De Miranda et al. 2010; Briseghella et al. 2010; Fa et al. 2016) to prove the feasibility of the proposed approach: assessing an almost complete FE model updating from ambient vibration data. In the first step, the authors carried out a variance-based sensitivity analysis (Saltelli and Sobol' 1995) of the cable forces to the bridge's significant inertial and stiffness parameters. The analyses proved that cable forces are mainly affected by the mass of the deck and the support deformability. This evidence enabled uncoupling the model updating in separate phases. There are multiple examples of FE model updating of cable-stayed bridges, but most of them are based on the sole experimental modal parameters (Zhang et al. 2001; Brownjohn and Xia 2000; Xiao et al. 2015; Zhu et al. 2015; Bursi et al. 2014; Lin et al. 2020a; Lin et al. 2020b; Ding and Li 2008; Pinqi and Brownjohn 2003; Park et al. 2015; Park et al. 2012; Ding and Li 2008). However, the FE updating of the cable forces is also a crucial task. As remarked by (Martins et al. 2020), 80% of research studies on cable-stayed bridges focus on cable forces optimization and control (Correia et al. 2020; Ferreira and Simoes 2011; Feng et al. 2022; Kim and Adeli 2005). Still, there are few pieces of research on the experimental evaluation of the cable forces (Cho et al. 2010; Haji Agha Mohammad Zarbaf et al. 2017; Nazarian et al. 2016; Feng et al. 2017; Haji Agha Mohammad Zarbaf et al. 2017), and a fewer on the model updating using both the modal parameters and the estimated cable forces (Hua et al. 2009). Nonetheless, the experimental assessment of the cable forces and the subsequent calibration of the forces predicted by the FE model is imperative to achieve a reliable prediction of the structural response.

Cable-stayed bridges, especially those built in the last decade, possess peculiar aesthetic and structural features. Cable-stayed bridges play a crucial role in infrastructure networks (Virlogeux 1999). However, they also characterize the urban landscape with their unique structural shape (Wilson and Liu 1991; Astaneh-Asl and Black 2001; Ni et al. 2019). There are multiple examples of cable-stayed bridges, but only some of them possess curved decks. The most known examples of cable-stayed bridges with a curved deck are: the Rhine bridge near Schaffhausen in Switzerland (Deger et al. 1996), the Safti Link bridge in Singapore (Brownjohn and Xia 2000), the twin bridges close to the Milan-Malpensa airport (Gentile and Martinez Y Cabrera 2004), the Katsushika bridge in Japan (Siringoringo and Fujino 2007), the Térénez bridge in France (Halpern and Billington 2013), the Yabegawa River Bridge (Kim and Lee 2012) and the Ponte del Mare bridge in Pescara (Italy) (Bursi et al. 2014; De Miranda et al. 2010). The deck curvature, despite its appreciated aesthetic peculiarities (Bonelli et al. 2010), adds complications in the construction phase and when assessing the actual structural behavior compared to cable-stayed bridges with a straight deck (Daniell and Macdonald 2007; Wen et al. 2016; Zhang et al. 2017; Martins et al. 2020). The selected bride also possesses an inclined tower to reduce the eccentricities of the cable forces. Therefore, especially for curved cable-stayed bridges, the experimental modal analysis is a determinant aspect for assessing the reliability of the structural model.

In (Briseghella et al. 2021), the authors discussed the dynamic characteristics of the bridge of Porto Marghera. Briseghella et al. (Briseghella et al. 2021) used the bridge's finite element (FE) model, calibrated to the experimental modal parameters, to assess the effect of its geometric configurations on its dynamic response. Specifically, the analyses aimed at determining the sensitivity of the natural frequencies to cable arrangement, deck curvature, and cross-section of the tower.

This paper represents an extension of the previous research (Briseghella et al. 2021) to discuss the feasibility of simultaneously calibrating an extended set of parameters affecting both the mass and stiffness features from ambient vibration data. Dynamic identification and FE model updating is a standard practice in structural engineering (Sehgal and Kumar 2016). However, the peculiarity of the Porto Marghera bridge also adds originality to this piece of research. The main aspects of novelty and originality are:

- Assessing the sensitivity of the cable forces and modal parameters to the structural parameters using a variance-based sensitivity analysis (Asgari et al. 2013).
- Proposing a step-wise procedure for the model updating of cable-stayed bridges using ambient vibration data and testing the updating procedure on the bridge of Porto-Marghera using two meta-heuristic optimization algorithms: the particle swarm optimization (PSO) and the differential evolution (DE).

- The authors found a significant discrepancy between the experimental and simulated cable forces in the preliminary FE model. The paper discusses the role of the bearing and tower stiffness in affecting the cable forces. These effects cannot be appreciated from the modal parameters of the deck.
- Highlighting the numerical issues related to the simultaneous identification of all the parameters from a single or multi-objective optimization problem. (Brincker et al. 2000).

The paper has the following organization. The second section briefly introduces the case study and the outcomes of operational modal analysis. The third section describes the FE model of the bridge and preliminary analysis to show the initial discrepancies with the experimental data. The fourth section discusses the sensitivity analysis of the cable forces to the inertial and stiffness parameters. The fifth section shows the results of the variance-based sensitivity analysis of the natural frequencies of the deck's stiffness in terms of Young's moduli of steel and concrete. The last section presents the global optimization results based on a step-wise approach.

PROBLEM FORMULATION

Ambient vibration tests of cable-stayed bridges can be used to obtain estimates of the modal parameters of the deck, the tower, and the stay-cables, which are the main components of a cable-stayed bridge. In OMA, the forces are unknown, therefore, the mode shapes cannot be mass normalized, and only the unscaled mode shapes can be determined for each mode (Parloo et al. 2001; Parloo et al. 2002; Parloo et al. 2003; Parloo et al. 2005; Brincker and Andersen 2003). However, in cable-stayed bridges, the forces can be effortlessly estimated from elementary mechanical models of the cables (Irvine 1981). Therefore, cable-stayed bridges represent a peculiar case where ambient vibration tests yield both the modal parameters and some forces acting in the structure. This paper shows that the augmented information due to cable forces might allow the complete model updating of the bridge model in terms of inertial and stiffness parameters. In conventional model updating from OMA, the scholar must select either the mass or stiffness matrix to be updated to avoid an ill-posed mathematical problem. As illustrated in Fig.1, the augmented information compared to traditional OMA allows the formulation of two objective functions in terms of cable forces and modal parameters, respectively. Fig.1 illustrates the procedure followed in this paper to understand whether the cable forces and the modal parameters can be used to achieve an almost complete FE model updating.

The authors are aware that each cable-stayed bridge is a stand-alone case. Therefore, it is challenging to generalize a model update using the cable forces, natural frequencies, and unscaled modal parameters. However, although each cable-stayed bridge might deserve minor adjustments to the procedure, this paper proves that it is possible to calibrate most of the parameters of the FE model, affecting both the mass and stiffness matrices. Specifically, except for the cables, each cable-stayed bridge consist of three main constituents: the tower, the deck, and the bearings. Intuition suggests the stiffness of the tower, bearings, and deck, and the mass of the deck influence both the modal parameters and the cable forces. It also indicates that the tower mass little affects the modal parameters and the stay-cables being a self-sustained structure.

Rigorously, a variance-based sensitivity analysis can highlight the most significant parameters affecting each cable force and modal parameter. As discussed in the body of the paper, the outputs of the sensitivity analysis prove that it is challenging to estimate all parameters at once since some parameters are more influential than others on a cable force or modal parameter. Therefore, the optimization problem formulation cannot be generalized and deserves a case-by-case analysis. However, as illustrated in Fig.1, the outputs from a sensitivity analysis and OMA can be used to select the parameters and properly formulate an optimization problem. Eq.(1) displays the general expression for the optimization problem, where $\boldsymbol{x}$ collects all the involved parameters affecting the deck, tower, and bearings.

$$\hat{\boldsymbol{x}} = \min_{\boldsymbol{x} \in \Omega} \{\boldsymbol{g}(\boldsymbol{x})\} \tag{1}$$

where $\hat{\boldsymbol{x}}$ and $\boldsymbol{x}$ collect the optimized and unknown parameters respectively, $\boldsymbol{g}$ the objective functions and Ω is the input space parameters. The objective function can be written by manipulating two functions containing the squared difference between the two types of input parameters.

$$\boldsymbol{g}(\boldsymbol{x}) = \begin{cases} \sum_{i=1}^{n_c} \left(\frac{T_i^m - T_i^c}{T_i^m}\right)^2, & \text{Cable forces} \\ \sum_{i=2}^{n_m} \left(\frac{\omega_i^m - \omega_i^c}{\omega_i^m}\right)^2 + \sum_{i=2}^{n_m} \left(1 - \text{diag}(\text{MAC}(\Phi_i^m, \Phi_i^c))\right), & \text{Modal parameters} \end{cases} \tag{2}$$

Where T_i^m and T_i^c are the measured and calculated cable forces, ω_i^m and ω_i^c are the measured and calculated natural pulsations, MAC is the Modal Assurance Criterion, Φ_i^m, and Φ_i^c are the measured and computed mode shapes, n_c is the number of cables, while n_m is the number of modes. The sensitivity analysis might indicate that some experimental parameters should be excluded from the objective function. Following a common approach in FE model updating, (Friswell and Mottershead 1995), meta-heuristic algorithms are used to solve the optimization. These techniques are mainly based on mimicking natural phenomena with simple iterative stochastic search rules in a phenomenological perspective, without a solid mathematical framework ensuring convergence to the global optima and its existence (Martí et al. 2018). Due to their intrinsic nature, does not exist a single unique method since the No-Free Lunch theorem (Wolpert and Macready 1997) affirms that there is no ideal algorithm to deal with any problem. However, their successful capability to handle complex problems without requiring any gradient-based information often represents the only means to deal with such situations (Martí et al. 2018). Indeed, meta-heuristic algorithms can accomplish the solution estimate of the optimal Pareto front for hard computational and multi-objective problems (Jones et al. 2002).

The general problem in Equation 2 is presented as a multiobjective optimization, where two objective functions to are optimized simultaneously. No single solution exists for a nontrivial multiobjective optimization problem that simultaneously optimizes each objective. The goal may be to find a representative set of Pareto optimal solutions and/or quantify the trade-offs in satisfying the different objectives. To simplify the problem, the authors conducted two separate single-objective optimizations in the following sections, as shown in Equations 5 and 8.

In this paper, the authors attempt to achieve the almost complete model updating of a cable-stayed bridge in Porto Marghera, selected as a case study, using experimental estimates of cable forces and modal parameters. The sensitivity analysis of each experimental parameter will support the formulation of the objective functions. However, despite multiple attempts, the optimization does not achieve convergence when a single objective function comprising all unknowns and experimental data is used. Despite several attempts, the authors will find that optimization is successful only if the optimization is split into three companion optimizations.

One for the tower stiffness using selected cable forces and modal parameters, one for the deck stiffness using selected modal parameters, and another for the vertical stiffness of the bearings using the deck mass and selected cable forces. By bearing, the authors intend the bridge component between the abutment and the deck. The selection of the cable forces and modal parameters for each optimization is based on the results of the sensitivity analysis.

This paper reveals the information obtained from a sensitivity analysis is necessary to achieve a mindful formulation of the objective function. Each cable stayed-bridge is a stand-alone case. However, the investigations prove that, under certain choices of objective functions, the problem can be considered well-posed and leads to the optimal set of parameters.

CASE STUDY

This section briefly describes the bridge and the experimental tests for characterizing its dynamic response.

Bridge description

The Porto Marghera bridge, connecting the city of Mestre to the Commercial Harbor of Venice-Marghera, Italy (Fig.2), has a total length of 387m, divided into six spans (42m + 105m + 126m + 30 + 42m + 42m). The first spans present a straight alignment, and the others a curved one with a 175m radius. Fig.3 shows the plan, elevation and typical cross-sections of the deck (De Miranda and Gnecchi-Ruscone 2010). The bridge is characterized by an inclined L-shape prestressed concrete tower, a single set of cables with a spatial arrangement and a curved steel-concrete composite deck (Briseghella et al. 2010). The two main spans have a cable-stayed structure with the stays arranged on a single plane, attached by the cross-section center. The bridge has two traffic lanes and pedestrian walkways with a 23.70m total width. The deck consists of a composite concrete-steel continuous girder embracing all six spans. There are two cross-sections of the deck, depicted in Fig.3. The first one, adopted by the end spans, consists of four double-T steel girders, while the second one, by the central spans, consists of two outer double-T steel girders and one central girder with a box section. Transverse crossbeams made by double-T beams spaced every 5.25m stiffen the girder. Steel girders and crossbeams have a 1.90m height and are connected to a cast-in-place concrete slab with a 25-27 cm thickness. The cast-in-place prestressed concrete inclined tower represents the bridge landmark and played a determining role in the conceptual and executive design of the bridge. The tower has about 75m in height, and a triangular cross-section characterizes its geometric layout. The cross-section base enlarges upward to provide a more suitable anchorage for the stays. The tower prestressing aimed at reducing the dead loads' eccentricity due to the curved deck layout. Despite the classic static scheme conception, typical of cable-stayed bridges with a central tower, numerous elements present a considerable architectonic impact and originality: the curvilinear layout of the suspended deck, the suspension scheme with a central curtain of stays, and the inclined tower with variable cross-section. Furthermore, the remarkable size of the deck made in the open profile (23.7m) and the mentioned bridge singularities supported the dynamic identification of the bridge for the experimental assessment of its dynamic response.

Dynamic characterization of the deck

The Laboratory of Vibrations and Dynamic Monitoring of Structures of Politecnico di Milano carried out the dynamic identification of the Porto Marghera bridge in two experimental campaigns during Autumn 2010 and Spring 2011 (Talebinejad et al. 2011; Yang et al. 2018). The two studies identified the modal parameters of the bridge and the natural frequencies and damping of the cable stays. The experimental modal analysis of the bridge was carried out using the Frequency Domain Decomposition (Brincker et al. 2000). The natural frequencies of the stays derived from the direct inspection of the auto spectra of the recorded signals (Bendat 1993). The details of the experimental tests and the results of dynamic identification are thoroughly discussed in (Briseghella et al. 2021). Concisely, the analysis identifies 12 and 11 modes in the 0-6Hz range during the experimental campaigns in 2010 and 2011 respectively. The authors selected the 11 experimental modes detected in 2011 for the sensitivity analysis and the following optimization. Tab.1 shows the experimental modal parameters. Fig.4 shows a representation of the mode shapes. The pictures include the tower and the stays, although the displayed modal deformations refer to the sole deck. As remarked in (Briseghella et al. 2021), the bending-torsional modes disavow the assumption of transversal non-deformability of the profile.

Dynamic characterization of the cables

Each cable stay was instrumented with a single sensor, placed at approximately 9.0m to the road surface. Additional details about the experimental setup are presented in (Briseghella et al. 2021; Zhao et al. 2020). Fig.6 and Tab.2 display the natural frequencies of the 18 stay cables identified in 2010 and 2011. Each figure reports the results of two symmetric stay cables, following the numbering in Fig.5. Fig.6 plots the natural frequencies and interpolating line n-f_n, where n is the mode order, and f_n is the associated natural frequency.

The interpolating line n-f_n displayed in Fig.6 does not exhibit a significant discrepancy to the single natural frequencies. Therefore, a simplified mechanical model of a fixed-fixed vibrating string can be used to derive the cable forces. The n-th natural frequency of a linear fixed-fixed string can be written as:

$$f_n = \frac{1}{2L}\left(\frac{T}{\rho}\right)^{0.5} \tag{3}$$

where L is the cable length, T is the cable force, ρ is the mass per unit of length of the cable. By assuming L, and ρ, the cable force can be estimated from the interpolating line n-f_n. Specifically, the cable force can be derived from the slope of the interpolating line as follows (Irvine 1981; Caetano et al. 2007):

$$T = \rho\left(2L\frac{\partial f_n}{\partial n}\right)^2 \tag{4}$$

where $\frac{\partial f_n}{\partial n}$ is the slope of the interpolating lines shown in Fig.6. Tab.3 and 4 list the estimated cable forces from the two experimental campaigns. As remarked in the original technical report, the recent publication (Briseghella et al. 2021) and past research on the cable force identification (Gentile and

Cabboi 2015), there is a certain discrepancy between the forces of two symmetric cables. However, there is a minor deviation to the n-f_n interpolation line. Therefore, the cable bending stiffness, sag extensibility, and intermediate springs do not play a significant role in affecting the cable forces (Mehrabi and Tabatabai 1998). The elementary model of a taut string can be considered valid in this case study and the observed differences between the experimental and numerical values reasonably depend on the structural parameters of the deck, tower, and supports. In the following sections, the authors will attempt to understand the possible reasons for the detected differences.

FINITE ELEMENT MODELLING OF THE BRIDGE AND PRELIMINARY ANALYSES

The FE model is developed in SAP200 and consists of 8014 nodes and 6600 elements (namely 2946 beams, 18 trusses, and 3636 solid elements), as depicted in Fig.7. The model is linear and does not reproduce any geometrical or mechanical non-linearity (Adeli and Zhang 1995; Song et al. 2007). In detail, four-node shell elements reproduce the concrete slab, while solid elements the tower. Rigid links, without mass, connected the concrete slab and the grid of steel stringers and transverse cross-beams. Additionally, rigid links reproduced geometrical offsets between the structural members and strut-and-tie bracings of the deck. The piers are modeled by 3D beam elements while the cables are modeled by cable elements. The bearings, not included in the original bridge model (Briseghella et al. 2021), are modeled by vertical linear spring. The model reproduces the curvature of the deck and the tower inclination. The initial values for the material properties are the following. The weight per unit volume and the Poisson's ratio of the concrete were assumed to be 25.0 kN/m^3 and 0.2, respectively. An additional weight equal to 1 kN/m^2 represented the deck slab, including the asphalt pavement and walkways. Young's modulus and steel weight was assumed to be 205 GPa and 785 kN/m^3 respectively.

Fig.8, Tab.6 and Tab.5 highlight the starting point of the model updating. Fig.8 plots all the eleven modes with an indication of the experimental and numerical natural frequencies and the MAC before calibration. Analogously, Tab.5 compares the experimental estimates of the cable forces and the FE model predictions before the updating. The numerical estimates of the cable forces (the cables are modeled as cable elements in SAP 2000) were obtained from static analysis under dead loads. The experimental forces were measured when the bridge was closed to vehicular traffic and only dead loads were acting on it. The authors do not adopt cable models with geometric nonlinearity for two main reasons. (i) The experimental estimates of the cable forces exhibit an almost exact agreement with the natural frequencies obtained from the classical linear model for a taut string. This observation proves that a nonlinear cable model might not be necessary for the current research objective. (ii) Secondarily, the authors are only considering ambient vibration tests, where the vibration amplitude of the cables is so low that geometric nonlinearities do not manifest. There is a significant gap in the starting point in terms of modal parameters and cable forces. The modal parameters exhibit an acceptable agreement before optimization. The cable forces are enormously biased. Therefore, a sensitivity analysis of the modeling parameters and cable forces is required to understand which parameters need to be updated.

Tab.7 shows the mass participation ratios of the considered eleven modes. The first six modes present quite relevant mass participating ratios, thus producing global mode shapes. On the contrary, the remaining modes approach zero percent of mass ratios, thus evidencing local modes as depicted in Fig.4. It is worth noting that modes 1, 3, 4, and 10 are clearly characterized by a single-direction mobilized mass, whereas modes 2, 5, and 6 are characterized by mixed mass participation ratios.

SENSITIVITY ANALYSIS OF THE CABLE FORCES

Before estimating the optimum values of the modeling parameters, sensitivity analyses provided a quantitative assessment of their effect on the chosen objective function and the mass and stiffness parameters. The authors chose as objective functions the 18 force values of the cables (nine on the Mestre side and nine on the Venice side) and an error function defined as the difference between the estimated and the numerical cable forces:

$$g_1 = \sum_{i=1}^{n_c} \left(\frac{T_i^m - T_i^c}{T_i^m} \right)^2 \tag{5}$$

where g_1 is the cost function, T_i^m the measured cable force, T_i^c the simulated cable force.

The analyses assessed the sensitivity of the objective functions to the parameters influencing the cable forces. The main parts of a cable-stayed bridge are the deck, the cables, the tower, and the supports. Each part possesses mass and stiffness properties. The cable forces are optimized by the designer to ensure the meeting of given design criteria generally in terms of stress and/or displacement. The physical parameters mainly affecting the actual value of cable forces are the mass and stiffness of the deck and the stiffness of the tower and the supports.

The tower's mass and bearings are self-sustained and have not been included. The geometry and material properties of the cables are known with high precision. Therefore, the authors will assume that they can be assumed as known in the sensitivity assessment. Young's modulus of steel is also known with significant accuracy and has not been included in the sensitivity assessment. The above considerations led to selection of five parameters representative of the deck's mass and stiffness, the tower's stiffness, and the bearings.

1. The Young's modulus of the tower ($E_{c,t}$). The cable forces might be significantly reduced if the tower is more deformable than expected by design. If so, the tower does not behave as almost fixed support for the cables. Therefore, Young's modulus of concrete has been chosen as a synthetic representation of the tower deformability. The bounds $[30, 50]$ GPa were assumed in the analyses.
2. The mass of the steel deck (ρ_s). The FE model accurately reproduces the geometry of the steel deck by using finite elements. However, the approximation related to finite elements might lead to an over or underestimation of the structural mass. Therefore, the weight per unit of volume of steel has been chosen to represent the mass of the steel deck. Indeed, ρ_s should be a known parameter since steel is manufactured in a workshop. As envisioned, the analysis shows that the parameter is negligible and can be excluded from the updating. The bounds $[75, 80]$ kN/m^3 were assumed in the analyses. The variability does not represent the possible variation of the steel mass but comprises the possible uncertainties related to the steel deck modeling.
3. The mass of the concrete deck (ρ_c). The FE model attempts to reproduce the geometry of the

concrete deck accurately. However, it is conventionally assumed that the concrete specific weight is equal to 25kN/m^3. Still, the weight of a reinforced concrete slab depends on the proportions of concrete and steel, which might cause variations of the conventional value assumed in calculations. Additionally, the uncertainties in the actual size of the concrete deck might propagate to the cable forces. Therefore, the authors selected the specific weight of concrete as a synthetic representative of the mass of the concrete deck. The uncertainties in the concrete deck's actual weight may depend on both the slab size and the specific weight of the concrete. The bounds $[24, 30]$ kN/m^3 were assumed in the analyses.

4. The Young's modulus of the concrete deck ($E_{c,d}$). The paper proposes a two-stage FE model update for cable-stayed bridges. In the first stage, the mass of the deck is estimated from the experimental values of the cable forces. In the second stage, the deformability of the deck is estimated from the experimental modal parameters. This approach works if the cable forces do not significantly depend on the deck stiffness. Therefore, Young's modulus of the concrete deck is used to prove that the cable forces are not affected by the deck stiffness. The bounds $[30, 50]$ GPa were assumed in the analyses.
5. The vertical stiffness of the bearings (k_a). The vertical stiffness of the bearings can be a crucial parameter affecting the cable forces. For example, the cable forces might increase significantly if the bearings are too deformable. The bounds $[10, 500]$ kN/mm were assumed in the analyses.

It must be remarked that the bounds of the parameters have been chosen so that the minimum never falls close to the bounds. The authors conducted several trial optimizations by progressively increasing the difference between the lower and upper bounds, initially close to the expected values corresponding to the physical variables the modeling parameters represent. Beyond a given increment of the bounds, the optimum parameters did not change and always fell within them. Therefore, after several attempts, the authors selected the limits specified above for running the optimization discussed in this paper. The boundaries which requested more attention and effort were those for the bearing stiffness, which are those characterized by the highest uncertainty since there was no preliminary experimental estimate of them. Therefore, the authors centered the boundaries at the nominal value of the bearing stiffness according to the producer and then increased the boundaries so that the minimum clearly fell within them. The analysis allowed decomposing the variance of the model's output (objective function and natural frequencies) into fractions that can be attributed to the chosen mechanical parameters (Pasca et al. 2021). The first step was setting the inputs sampling range and generating the model inputs according to Saltelli's sampling scheme (Saisana et al. 2005). ($N \cdot (2D + 2)$ model inputs were generated, where $N = 100$ is the number of samples, and $D = 2$ is the number of input parameters). After running all the model inputs, the first order was calculated. The authors computed the first-order sensitivity indexes (S_1), which do not consider interactions among input variables (Sobol' 1990). Instead, they contribute to the output variance of the chosen objective function of a given modeling parameter (Young's modulus, mass density, e.g.) (Aloisio et al. 2020; Aloisio et al. 2021; Aloisio et al. 2022a; Aloisio et al. 2022b). S_1 measures the effect of varying each parameter alone, averaged over variations of the other input parameters. Theoretically, the summation of all indexes is one. However, the sensitivity analysis is based on a Montecarlo approach. Therefore, the sum of all indexes tends to be one, but it is not precisely one due to the statistical approach followed for their estimation. Tab.8,9 list the sensitivity indicators of the objective function and cable forces respectively, where the rows refer to different parameters.

The objective function in Eq.(3), later used for the optimization of cable forces, comprises the modeling errors of all cables, although each cable is more affected by a specific set of variables among the chosen five. The results show that the most significant variable is the vertical stiffness of the bearings. In the original model developed by the authors (Briseghella et al. 2021), the bearings were assumed as fixed supports since their stiffness did not cause a significant effect on the modal parameters. Conversely, the cable forces are significantly influenced by k_a, as proved by the sensitivity indicator, reaching approximately 94%. In this preliminary phase, the authors assumed a range of stiffness to have a maximum vertical displacement of 1mm. The other significant parameters, with sensitivity indicators of approximately 5%, are Young's tower modulus and the concrete deck's mass. The authors expected the importance of the two parameters, compared to the steel mass and Young's modulus of the concrete deck, which have a minor influence on the cable forces. The results in Tab.8 indicate that the vertical stiffness will be the most influential parameter in the FE updating of the cable forces.

Parallelly, Tab.9 displays the contribution of each of the five parameters to the force values of the nine cables on the Mestre and Venice sides. The results are almost identical for the two sides, despite minor discrepancies. The tower deformability influences the force in the shortest cable close to the tower. The sensitivity indicator reaches almost 85%. The mass of the concrete deck influences its value by nearly 15%, while the bearings, quite distant from the cables, do not sensibly affect the force value.

The sensitivity indicators start modifying in favor of the concrete deck's mass and the subsequent cables' bearing stiffness. The middle cables exhibit the highest sensitivity to the deck mass, reaching more than 90% in some cases. Conversely, the cables closest to the bearings (especially the ultimate three) exhibit the highest sensitivity to the bearing supports, close to 90%.

In conclusion, the outcomes of the sensitivity analyses on the single cable forces highlight three trends for the $E_{c,t}$, ρ_c, and k_a. First, the tower deformability exhibits the highest effects on the shortest cable. Then its effects decrease to the ninth cable with an almost null effect. The mass of the concrete deck shows a sensitivity growth starting from the shortest to the middle cables. Then, the effects decrease for the cables close to the supports. The sensitivity indicators to the bearings' stiffness grow to a maximum for those cables closest to the supports.

Fig.9,10 and 11 provide a graphical illustration of the outcomes of the sensitivity analysis by means of a scatter plot of the objective functions in the considered space of parameters. The representation has been limited to $E_{c,t}$, ρ_c, and k_a, which play the most significant role.

Fig.9 shows two representations of the scatter plot of the objective function in Eq.(3). The objective function reduces significantly if the k_a is lower than 100 kN/mm. For higher values of k_a, the objective function tends to stabilize. This effect is reasonable. Due to a lower deformation, the supports tend to behave rigidly and play a minor role in the cable forces. The alternate dots' color evidences the presence of a maximum for the ρ_c value.

Fig.10,11 illustrate the effects of $E_{c,t}$, ρ_c and k_a on each cable force on the Mestre and Venice sides. The plots confirm the results in Tab.9. The shortest cables exhibit a prevalent dependence on the stiffness of the tower. If Young's modulus $E_{c,t}$ grows to values higher than 30MPa, the objective function reduces. Conversely, the objective function stabilizes at a higher value as the tower's stiffness lowers. If the tower does not deform, it behaves as a rigid support for the cables. The second and third cables start manifesting an inversion of the objective function dependence since the weight of the concrete deck leads to a higher dispersion of the dots towards lower values of the objective function. Starting from the fourth cable, the dependence of the objective function on k_a starts displaying. Specifically, moving from the fourth to the ninth cable, the surfaces tend to reduce in the vertical scatter related to the concrete specific weight and exhibit a clear dependence on k_a. Expressly, the curves referred to as the ninth cables have a nonlinear trend, where the objective function reduces for lower values of the bearing stiffness.

The plots in Fig.10,11 are proxies for assessing the role of the parameters in finding the optimal set associated with the minimum of the objective function in Eq.(3). The optimal set of parameters is associated with higher values of Young's modulus of the tower ($E_{c,t} > 30$MPa), a lower value of the concrete mass of the deck ($\rho_c < 25$kN/m^3), and a lower value of the bearing stiffness ($k_a < 100$kN/mm).

SENSITIVITY ANALYSIS OF THE MODAL PARAMETERS

To measure the distance between the estimated and the numerical modal parameters, the following objective function is used:

$$f(\boldsymbol{x}) = f_1(\boldsymbol{x}) + f_2(\boldsymbol{x}) \tag{6}$$

$$f_1(\boldsymbol{x}) = \sum_{i=1}^{n_m} \left(\frac{\omega_i^m - \omega_i^c}{\omega_i^m} \right)^2 \tag{7}$$

$$f_2(\boldsymbol{x}) = \sum_{i=1}^{n_m} \left(1 - \mathrm{diag}(\mathrm{MAC}(\Phi_i^m, \Phi_i^c))\right) \tag{8}$$

where $f(\boldsymbol{x})$ is the cost function, $\boldsymbol{x}$ is the vector collecting all the modeling parameters, $f_1(\boldsymbol{x})$ and $f_2(\boldsymbol{x})$ the cost functions in terms of natural frequencies and mode shapes, ω the natural pulsation, the apex $(*)^m$ indicates a measured variable, the apex $(*)^c$ a calculated variable, Φ_i is the mode shape vector, n_m is the number of modes, MAC is the Modal Assurance Criterion.

The main aspects arising from the observation of the sensitivity analysis might be itemized as follows based on the results collected in Tabs.10,11,12:

- Tab.10-The vertical stiffness of the bearing is the most influential parameter in Eq.(6). However, as shown in Tab.10, the highest sensitivity to the bearing stiffness is given by the cost function in terms of mode shapes ($\approx$ 97.2%). Conversely, the cost function in terms of natural frequencies is more affected by the mass of the deck (ρ_c), with an approximate 61.4% indicator. In the selected ranges of variation, the weight per volume of steel does not sensibly affect the objective functions with a sensitivity indicator less than 0.1%.
- Tab.11-The sensitivity analysis of each natural frequency confirms the minimal effect of the weight per unit of volume of steel. Conversely, there are several cases where Young's modulus of the tower and the deck and mass per unit of volume of concrete are more influential than the bearing stiffness. This fact can be mainly observed for modes V2, V3, T1, and T2. Specifically, V2 exhibits a marked dependence on $E_{c,t}$ ($\approx$ 49.6%), ρ_c ($\approx$ 25.4%), and k_a ($\approx$ 74.1%). Modes V3, T1, and T2 also significantly depend on Young's modulus of the deck, with sensitivity indicators approximately equal to 16.3%, 58.3%, and 48.8%, respectively. These are the only cases where Young's modulus of the deck is influential. Therefore, V3, T1, and T2 are the only modes that can be ideally used to estimate Young's modulus of the deck. Except for the mentioned modes, the other modes exhibit a prevalent dependence on the bearing stiffness.
- Tab.12-The results in natural frequencies are pretty similar to those in MAC. The main difference stands in the role of the mass per unit of volume of concrete. In comparison, ρ_c and k_a are the most influential parameters for the natural frequencies, except for V2,

V3, T1, and T2 modes. The sole bearing stiffness is the most significant parameter with a sensitivity higher than 90%. Similarly, V2, V3, and T1 also show a clear dependence on Young's modulus of the tower. In contrast, V3, T1, and T2 also depend on Young's modulus of the deck.

On average, the sensitivity ranking of the selected parameters from the most influential to the less is: bearing stiffness (k_a), weight per unit of volume of concrete (ρ_c), Young's modulus of the tower ($E_{c,t}$), Young's modulus of the deck ($E_{c,d}$), and the weight per unit of volume of steel. In general, the parameters are highly correlated since the sum of the sensitivity indicators in Tabs.10,11,12 is much higher than 100%. This fact depends on including mass and stiffness parameters in the sensitivity analysis. Figs.12-13 show selected scatter plots of the simulated data as a function of the three most influential parameters, the bearing stiffness, Young's modulus of the tower, and the mass per unit of volume of concrete.
Differently from the scatter plots of the cable forces' sensitivity analysis, the current ones manifest the presence of subspaces where dots coalesce. The shape of the objective functions, the one in Eq.(6) and those representatives of the frequency and MAC contributions stand on the same hyper-surface. They all prove a lowering of the objective function as the bearing stiffness rises and the concrete mass lowers. Other aspects cannot be interpreted from a direct inspection of the scatter plots of the three objective functions in Fig.12. The dots associated with the same realizations but corresponding to each mode aggregate peculiarly, exhibiting discontinuities like for V3 and VT1, local minima like for M1 and T2, and stationary regions where the variation of the parameters is not influential.

Discussion

The selected plots show the complexity of a possible model update driven by the modal parameters. There are two main reasons. (i) The preliminary model of the bridge without updating already exhibits an excellent agreement with experimental data. Therefore, the parameter calibration should lead to the near identity between the experimental and numerical modal parameters.

However, the model updating using both the mass and stiffness parameters would be indeterminate, and the scholar should arbitrarily assume one parameter possibly associated with lower uncertainty. (ii) The presence of subspaces and discontinuities in the plots of either the natural frequency or the mode shape prove the possible limits of a meta-heuristic optimization algorithm. The optimization outcome depends on the subspace where the algorithm might fall in the search process. Therefore, a FE model updating using the cable forces has several advantages compared to one based on the modal parameters.

The simulated cable forces are in lousy agreement with the experimental ones. Therefore, a model update using the cable forces would be more valuable than one based on the modal parameters, which are already in excellent agreement. Specifically, the parameters affecting the cable forces are not highly correlated. Therefore, a lower number of parameter subsets is associated with a good matching with the experimental data. In contrast, the parameters affecting the modes are highly correlated. This fact leads to higher parameter subsets related to an excellent agreement with the experimental data.

The objective functions of cable forces have a regular trend without discontinuities. Conversely, the presence of multiple subspaces collecting the modal parameters might compromise the success of the search process of optimization algorithms.

The cable forces T1,M1 and T2,M2 can be used to estimate $E_{c,t}$ ($S_w > 50\%$), the remaining cable to estimate ρ_c ($S_w > 50\%$) and k_a ($S_w > 50\%$). The sole parameter left is $E_{c,d}$ which can be estimated from an objective function in terms of cable T1, and mode shapes excluding the second one, mainly affecting the tower deformability.

FE MODEL UPDATING

Multiple attempts were carried out to test the feasibility of a global optimization algorithm where all the parameters are updated simultaneously. However, all the efforts were unsuccessful. The parameters are highly correlated, and the objective functions, especially those dependent on the modal parameters, present many local minima. Therefore, simultaneously updating all the parameters using meta-heuristic algorithms is challenging. Furthermore, the algorithms always select the lower or upper bounds of the parameter domain. Thus, the following is the unique updating procedure that provided optimum parameters within the bounds and in good agreement with the experimental data. The main drawback of the procedure is the assumption of specific parameters in the first optimization steps. However, as proved by the sensitivity analysis, different choices of the assumed parameters, namely $E_{c,t}$ and $E_{c,d}$, do not modify the optimization outputs, with differences lower than 5%. Therefore, the sole successful optimization will be described and discussed in this section. The optimization process is based on the following steps:

1. Optimization of ρ_c and k_a, after assuming a specific value for Young's moduli of the tower $E_{c,t}$ and the deck $E_{c,d}$. The objective function depends on all the cable forces except for T1, M1, and T2, M2.
2. Optimization of Young's modulus of the concrete tower ($E_{c,t}$), after assuming ρ_c and k_a from the first step and Young's modulus of the deck $E_{c,d}$. The objective function depends on the cable forces T1, M1 and T2, M2, and the second mode shape.
3. Optimization of Young's modulus of the concrete deck ($E_{c,d}$), after assuming ρ_c, k_a and $E_{c,d}$, from the previous optimization steps.

The global optimization algorithms, the differential evolution (DE) (Storn and Price 1997) and the particle swarm optimization (PSO) (Kennedy and Eberhart 1995), are used for mutual validation. Also, to perform the model updating, the script is written in Python using SAP2000 OAPI with the Python module Scipy (to run DE) and PySwarms (Miranda 2018) (to run PSO). Since no significant difference is observed in comparing the outcomes of the two optimization algorithms, the authors will only report the results from PSO. In detail:

1. **Optimization of ρ_c and k_a**: This optimization can be formulated as unconstrained and single-objective since there is one Objective Function (OF) $g(\boldsymbol{x})$ to be minimized and no equality or inequality constraints. The problem can be formulated as follows:

$$\hat{\boldsymbol{x}}_1 = \min_{\boldsymbol{x}_1 \in \Omega_1} \{g_1(\boldsymbol{x}_1)\} \tag{9}$$

$$g_1(\boldsymbol{x}_1) = \sum_{i=3}^{9} \left(\frac{T_i^m - T_i^c}{T_i^m}\right)^2 \;\; \boldsymbol{x}_1 = \{\rho_c, k_a\}^T, \; \hat{E}_{c,t} = \hat{E}_{c,d} = 30\text{GPa} \tag{10}$$

The objective functions include all the nine cable forces on the Venice and Mestre sides except for the two close to the tower mainly affected by $E_{c,t}$. The search domain is a multidimensional space Ω, based on the admissible intervals of values for each j-th variable, defined by its lower and upper bounds $[x_j^l, x_j^u]$. This detects a box-type hyper-rectangular search space Ω which is typically defined as the Cartesian product (denoted by the $\times$ symbol) among the admissible intervals

$$\Omega = [\rho_c^l, \rho_c^u] \times [k_a^l, k_a^u] \tag{11}$$

2. **Optimization of $E_{c,t}$** This optimization can be formulated as unconstrained and single-objective, since there is one Objective Function (OF) $g(\boldsymbol{x})$ to be minimized and no equality or inequality constraints.

$$\hat{\boldsymbol{x}}_2 = \min_{\boldsymbol{x}_2 \in \Omega_2} \{g_2(\boldsymbol{x}_2)\} \tag{12}$$

$$g_2(\boldsymbol{x}_2) = \sum_{i=1}^{2} \left(\frac{T_i^m - T_i^c}{T_i^m}\right)^2 + \sum_{i=2}^{2} \left(\frac{\omega_i^m - \omega_i^c}{\omega_i^m}\right)^2 + \sum_{i=2}^{2} \left(1 - \text{diag}(MAC(\Phi_i^m, \Phi_i^c))\right) \tag{13}$$

$$\boldsymbol{x}_2 = \{E_{c,t}\}^T, \; \hat{E}_{c,d} = 30\text{GPa}, \; \{\hat{\rho}_c, \hat{k}_a\}^T \text{ in Tab.13 and 14} \tag{14}$$

The objective functions include two cables on the Venice and Mestre sides close to the tower and the second mode shape associated with the tower deformation.

3. **Optimization of $E_{c,d}$**: This optimization can be formulated as unconstrained and single-objective since there is one Objective Function (OF) $g(\boldsymbol{x})$ to be minimized and no equality

or inequality constraints.

$$\hat{\boldsymbol{x}}_3 = \min_{\boldsymbol{x}_3 \in \Omega_3} \{g_3(\boldsymbol{x}_3)\} \tag{15}$$

$$g_3(\boldsymbol{x}_3) = \sum_{i=1,3}^{12} \left(\frac{\omega_i^m - \omega_i^c}{\omega_i^m}\right)^2 + \sum_{i=1,3}^{12} \left(1 - \mathrm{diag}(MAC(\Phi_i^m, \Phi_i^c))\right) \tag{16}$$

$$\boldsymbol{x}_3 = \{E_{c,d}\}^T, \;\; \{\hat{\rho}_c, \hat{k}_a, \hat{E}_{c,t}\}^T \text{ in Tab.13 and 14} \tag{17}$$

The objective functions includes all mode shapes except for the second one related to the tower deformation.

It must be remarked that beyond its strictly physical meaning, concrete Young's modulus should be also considered as a modeling parameter (Schlune et al. 2009). Indeed, in the FE model updating procedures, the concrete Young's modulus is often assumed as a single parameter describing the dynamical stiffness adaptation for all directions simultaneously, thus strongly affecting the simulated global dynamics of the FE model (Schlune et al. 2009). Therefore, since it summarizes different contributions to the global simulated dynamic response, it is affected by an intrinsic severe level of uncertainty (Schlune et al. 2009). Firstly, these uncertainties may be related to modeling errors, e.g. due to simplified assumptions when modeling complex structures, or from actual intrinsic factors, such as the mesh discretization level (Park et al. 2012). Secondly, they may be also related to model parameter errors, i.e. due to material and geometric properties uncertainties, as well as a proper definition of their variation range boundaries (Brownjohn and Xia 2000). These boundaries are normally set for the purpose of avoiding physically impossible updated parameter outcomes. However, a trade-off between physically acceptable parameter values and the convergence level is often required (Brownjohn and Xia 2000). In addition, the after-updating concrete stiffness parameters are usually expected to increase because, by definition, the dynamic Young's modulus of concrete is greater than the static one (Jaishi and Ren 2005). Another reasonable concomitant cause is related to concrete long-term hardening phenomena (Schlune et al. 2009). Thus, in (Daniell and Macdonald 2007) it is suggested to adopt an already significant value for the concrete Young's modulus initial values, e.g. about 37 GPa. From this value, it is expected at least an incremental variation at least of 15% (Park et al. 2012). However, after-updating values may also reach considerably high values, e.g. about 53 GPa, as demonstrated in (Jaishi and Ren 2005). In summary, due to epistemic uncertainty, the tuning parameters, generally Young's moduli, not only express their intrinsic physical meaning, characterized by specific acceptable values. First, they are modeling parameters that collect and compensate for modeling errors in the optimization phase, while reducing the discrepancy between the simulated and experimental dynamic response. Therefore, for the above-mentioned reasons, the authors selected wide boundaries for Young's moduli for both the sensitivity analysis and the optimization.

The three optimizations led to the following values of the objective functions: 0.4306, 0.0347 and 1.0296 corresponding to Eq.(10), (13) and (16), respectively. Multiple identical repetitions of the optimization gave the same results. Tab.13 and 14 show the results of the three optimizations in a single table, displaying the values of the cable forces and modal parameters before and after the updating. Additionally, Tab.13 and 14 show the optimum parameters and the relative upper and lower bounds.

The updating reveals that, while the agreement between modal parameters does not improve meaningfully, the comparison in terms of cable forces enhances significantly. Except for cable two on both the Mestre and Venice side, the relative average error reduces from -17% to -6%. The key to successful updating is introducing the bearing stiffness.

Initial updating attempts excluded the bearing stiffness and always led to minor improvements in the matching between cable forces. However, the agreement's progress in modal parameters is negligible and worsens in some cases. This fact proves that the geometric features are more influential on the modal parameters than the chosen updated parameters. The average frequency error is approximately 1% before and after updating. The same for the average MAC, which keeps constant at 90%. The values of the optimum parameters are consistent with the engineering judgment. For example, the optimum concrete mass is 24kN/m^3, while Young's modulus of the deck is 40GPa. The optimum Young's modulus of the tower is higher than the values expected for concrete, being equal to 61.1GPa. This value proves that the tower exhibits a higher stiffness. Higher stiffness might be related to modeling errors in the actual geometry and possible discrepancies between the design and real tower geometry.

As recalled by (De Miranda and Gnecchi-Ruscone 2010), the bearings of the considered structure were produced by TENSA and consist of laminated neoprene pads. The stiffness of the bearings significantly influences the global dynamic behavior in terms of torsional and horizontal modes and cable forces. The bearings, modeled as linear springs, possess a high level of uncertainty. As noted by (Petersen and Øiseth 2017; Petersen et al. 2018), the uncertainty depends not only on the neoprene material itself but also on unknown effects related to the embedded steel plates and pre-tensioning. Secondarily, the idealization of a bearing as a single node can also cause errors (Zhu et al. 2019). The optimum value of the bearing stiffness is 1350kN/mm. The vertical stiffness falls within the expected range of stiffness for this kind of support (Kaczinski et al. 2016; Zhang and Xie 2019). The average expected deformation of the bearing without traffic loads equals 5.78mm. Tab.15 shows the reaction forces at the supports corresponding to fixed and deformable supports. While the bearing stiffness significantly affects the cable forces and the modal parameters, it does not influence the reaction forces. In particular, the reaction forces exhibit minor relative discrepancies, approximately 1%.

The results of the updating are consistent with the ones discussed in (Briseghella et al. 2021). Briseghella et al. found that the optimum matching is achieved when $E_{c,t} = 41.67$Gpa and $E_{c,d} = 33.74$Gpa. The introduction of the bearing stiffness within the updating process lead to an increment of the optimum values, equal to $E_{c,t} = 51.1$Gpa and $E_{c,d} = 40$Gpa, as shown in Tab.13 and 14. Still, it is challenging to understand the mechanical reasons behind the observed, despite minor differences. Plausibly, the bearing stiffness adds higher deformability to the structure, which is compensated by a stiffer deck and tower, a consequent higher $E_{c,d}$ and $E_{c,t}$. For optimization tasks considering non-linear problems, derivative- free global algorithms are particularly suitable (Hofmeister et al. 2019)

As already mentioned before, it must be remarked that Young's moduli of concrete of the FE model should not be considered strictly physical quantities, but, indeed, modeling parameters

(Schlune et al. 2009). Due to epistemic uncertainty, the FE model might not represent the actual structure. Therefore, the tuning parameters, generally Young's moduli, not only express their intrinsic physical meaning, characterized by specific acceptable values. First, they are modeling parameters that collect and compensate for the modeling error in the optimization phase (Jaishi and Ren 2005; Park et al. 2012). Therefore, it generally happens that the values of Young's moduli might exceed or underestimate the expected values for concrete (Schlune et al. 2009; Brownjohn and Xia 2000). Therefore, the authors selected wide boundaries for Young's moduli for both the sensitivity analysis and the optimization (He et al. 2022).

CONCLUSIONS

This paper presents and discusses the almost complete finite element model updating of cable-stayed bridges using modal parameters and cable forces estimates. The optimization problem is particularly challenging when dealing with large-scale structures with numerous degrees of freedom using traditional model updating methods. For this reason, several scholars use surrogate models to reduce computational costs, like the response surface (RS) method (Fang and Perera 2009; Fang and Perera 2011; Horta et al. 2011). However, if a preliminary sensitivity analysis is carried out to support the mindful formulation of the objective functions, the traditional model updating based on meta-heuristic optimization algorithms represents a feasible approach. In this paper, the authors achieve the almost complete model updating of a cable-stayed bridge following a step-wise procedure supported by extensive variance-based sensitivity analyses.

The procedure was applied to a cable-stayed bridge with a curved deck and inclined tower in Porto Marghera (Italy). The authors used the particle-swarm (PSO) and differential evolution (DE) algorithms to calibrate the model parameters from ambient vibration data collected on the deck and cables. The availability of the cable forces estimates allows updating the inertial and stiffness features, compared to more conventional FE updating where the sole modal parameters impose the updating of either the mass or stiffness matrix to avoid ill-posedness and indeterminacy of the optimization problem. The paper highlights the importance of preliminary sensitivity analyses to formulate the optimization problem correctly. In the considered case study, preliminary sensitivity analyses showed that the most influential parameters to be included in the update are: the concrete mass (ρ_c), Young's modulus of the concrete deck ($E_{c,d}$), Young's modulus of the concrete tower ($E_{c,t}$), and the bearing stiffness (k_a). The sensitivity analyses demonstrated that ρ_c and k_a are mainly affected by the cable forces, except for the cables close to the tower. The tower's deformability ($E_{c,t}$) mainly influences the cables close to the tower. At the same time, the modal parameters are mainly influenced by Young's modulus of the deck, except for the second mode related to the tower deformation. Therefore, this evidence supported a three-step model updating, leading to the progressive optimization of ρ_c and k_a, then $E_{c,t}$ and ultimately $E_{c,d}$. The updating in the first two steps required the assumptions of specific parameter values. However, the optimization results are not notably affected by different parameter choices, as confirmed by the sensitivity analysis. The authors attempted the optimization of all the parameters simultaneously, following multi-objective and single-objective approaches. However, all the endeavors were unsuccessful since the algorithm always selected optimum values corresponding to the lower and upper bounds. As evidenced by the sensitivity analysis, the chosen objective functions, especially the one in modal parameters, present several local minima/maxima regions, which undermine the success of global optimization, including all the parameters. Therefore, the only procedure which led to values within the confidence bounds is the three-step one discussed in this paper. The analyses also reveal that the agreement between modal parameters does not improve significantly. The average percentage error remains equal before and after the update. Conversely, the cable forces exhibited a noteworthy improvement. The key to this improvement is the introduction of bearing stiffness. The sensitivity analysis highlighted the influence of the bearing stiffness on the modal parameters and cable forces. The bearings consist of layered neoprene pads with an estimated vertical stiffness equal to 1350kN/mm, consistent with the vertical stiffness of these structural devices. This paper establishes that meta-heuristic optimization algorithms can be challenging to use in FE model updating of cable-stayed bridges, especially when many parameters need to be optimized. Therefore, the scholar must steer the optimization process by limiting the search space and devising step-wise methods. A sensitivity analysis represents a necessary step to correctly isolate the most relevant unknown parameters and suitably formulate the sets of objective functions to be optimized.

DATA AVAILABILITY STATEMENT

All data, models, or code that support the findings of this study are available from the corresponding author upon reasonable request.

ACKNOWLEDGEMENTS

The authors would like to thank the technical personnel (M. Antico and M. Cucchi) of the VIBLAB Laboratory of Vibrations and Dynamic Monitoring of Structures, Polytechnic of Milan, for their valuable help in conducting the field tests. Moreover, the collaboration of Dr. Fulvio Busatta (University of Cape Town) in implementing the first Finite Element Model and of Prof. Airong Chen (Tongji University) in performing a Risk Analysis of the Bridge is highly acknowledged. This work was supported by the National Natural Science Foundation of China [grant No. 51778148].

DISCLOSURE STATEMENT

No potential competing interest was reported by the authors.

FUNDING

The authors gratefully acknowledge the financial support from the National Natural Science Foundation of China (Grant No. 51778148).

REFERENCES

Adeli, H. and Zhang, J. (1995). "Fully nonlinear analysis of composite girder cable-stayed bridges." *Computers & structures*, 54(2), 267–277.

Aloisio, A., Alaggio, R., and Fragiacomo, M. (2021). "Bending stiffness identification of simply supported girders using an instrumented vehicle: full scale tests, sensitivity analysis, and discussion." *Journal of Bridge Engineering*, 26(1), 04020115.

Aloisio, A., Di Battista, L., Alaggio, R., and Fragiacomo, M. (2020). "Sensitivity analysis of subspace-based damage indicators under changes in ambient excitation covariance, severity and location of damage." *Engineering Structures*, 208, 110235.

Aloisio, A., Pasca, D. P., Di Battista, L., Rosso, M. M., Cucuzza, R., Marano, G. C., and Alaggio, R. (2022a). “Indirect assessment of concrete resistance from fe model updating and young’s modulus estimation of a multi-span psc viaduct: Experimental tests and validation.” *Structures*, Vol. 37, Elsevier, 686–697.

Aloisio, A., Rosso, M. M., and Alaggio, R. (2022b). “Experimental and analytical investigation into the effect of ballasted track on the dynamic response of railway bridges under moving loads.” *Journal of Bridge Engineering*, 27(10), 04022085.

Arangio, S. and Bontempi, F. (2015). “Structural health monitoring of a cable-stayed bridge with bayesian neural networks.” *Structure and Infrastructure Engineering*, 11(4), 575–587.

Asgari, B., Osman, S., and Adnan, A. (2013). “Sensitivity analysis of the influence of structural parameters on dynamic behaviour of highly redundant cable-stayed bridges.” *Advances in Civil Engineering*, 2013.

Astaneh-Asl, A. and Black, R. G. (2001). “Seismic and structural engineering of a curved cable-stayed bridge.” *Journal of Bridge Engineering*, 6(6), 439–450.

Babajanian Bisheh, H., Ghodrati Amiri, G., Nekooei, M., and Darvishan, E. (2019). “Damage detection of a cable-stayed bridge using feature extraction and selection methods.” *Structure and Infrastructure Engineering*, 15(9), 1165–1177.

Bendat, J. S. (1993). “Spectral techniques for nonlinear system analysis and identification.” *Shock and Vibration*, 1(1), 21–31.

Bernal, D. (2004). “Modal scaling from known mass perturbations.” *Journal of Engineering Mechanics*, 130(9), 1083–1088 cited By 81.

Bernal, D. and Gunes, B. (2002). “Damage localization in output-only systems: A flexibility based approach.” *IMAC-XX*, 1185–1191 cited By 6.

Bonelli, A., Bursi, O., Ceravolo, R., Santini, S., Tondini, N., and Zasso, A. (2010). “Dynamic identification and structural health monitoring of a twin deck curved cable-stayed footbridge: the “ponte del mare” of pescara in italy.” *Proceedings of the 5th European Workshop on Structural Health Monitoring*, Sorrento, Italy, 370–375.

Brandt, A., Berardengo, M., Manzoni, S., Vanali, M., and Cigada, A. (2019). "Global scaling of operational modal analysis modes with the omah method." *Mechanical Systems and Signal Processing*, 117, 52–64.

Brincker, R. and Andersen, P. (2003). "A way of getting scaled mode shapes in output only modal analysis." *Proceedings of XXI International Modal Analysis Conference*, 141–145 cited By 117.

Brincker, R., Rodrigues, J., and Andersen, P. (2004). "Scaling the mode shapes of a building model by mass changes." *Proceedings of the 22nd International Modal Analysis Conference (IMAC)*, 119–126 cited By 22.

Brincker, R., Zhang, L., and Andersen, P. (2000). "Modal identification from ambient responses using frequency domain decomposition." *Proc. of the 18*'International Modal Analysis Conference (IMAC), San Antonio, Texas*.

Briseghella, B., Fa, G., Aloisio, A., Pasca, D., He, L., Fenu, L., and Gentile, C. (2021). "Dynamic characteristics of a curved steel–concrete composite cable-stayed bridge and effects of different design choices." *Structures*, Vol. 34, Elsevier, 4669–4681.

Briseghella, B., Siviero, E., Lan, C., Mazzarolo, E., and Zordan, T. (2010). "Safety monitoring of the cable stayed bridge in the commercial harbor of venice, italy." *Bridge Maintenance, Safety, Management and Life-Cycle Optimization: Proceedings of the Fifth International IABMAS Conference, Philadelphia, USA, 11-15 July 2010*, CRC Press, 379.

Brownjohn, J. M. and Xia, P.-Q. (2000). "Dynamic assessment of curved cable-stayed bridge by model updating." *Journal of structural engineering*, 126(2), 252–260.

Bursi, O. S., Kumar, A., Abbiati, G., and Ceravolo, R. (2014). "Identification, model updating, and validation of a steel twin deck curved cable-stayed footbridge." *Computer-Aided Civil and Infrastructure Engineering*, 29(9), 703–722.

Caetano, E., Silva, S., and Bateira, J. (2007). "Application of a vision system to the monitoring of cable structures." *Seventh international symposium on cable dynamics*, Citeseer, 225–236.

Cho, S., Lynch, J. P., Lee, J.-J., and Yun, C.-B. (2010). "Development of an automated wireless tension force estimation system for cable-stayed bridges." *Journal of Intelligent Material Systems* *and Structures*, 21(3), 361–376.

Correia, J., Ferreira, F., and Maçãs, C. (2020). “Cable-stayed bridge optimization solution space exploration.” *Proceedings of the 2020 Genetic and Evolutionary Computation Conference Companion*, 261–262.

Daniell, W. E. and Macdonald, J. H. (2007). “Improved finite element modelling of a cable-stayed bridge through systematic manual tuning.” *Engineering Structures*, 29(3), 358–371.

De Miranda, M., De Palma, A., and Zanchettin, A. (2010). ““ponte del mare”: Conceptual design and realization of a long span cable-stayed footbridge in pescara, italy.” *Structural engineering international*, 20(1), 21–25.

De Miranda, M. and Gnecchi-Ruscone, E. (2010). “Construction of the cable-stayed bridge in the commercial port of venice, italy.” *Structural Engineering International*, 20(1), 13–17.

Deger, Y., Cantieni, R., and de Smet, C. (1996). “Finite element model optimization of the new rhine bridge based on ambient vibration testing.” *Balkema Publishers(Netherlands),*, 817–822.

Ding, Y. and Li, A. (2008). “Finite element model updating for the runyang cable-stayed bridge tower using ambient vibration test results.” *Advances in Structural Engineering*, 11(3), 323–335.

Fa, G., He, L., Fenu, L., Mazzarolo, E., Briseghella, B., and Zordan, T. (2016). “Comparison of direct and iterative methods for model updating of a curved cable-stayed bridge using experimental modal data.” *Proceedings of the IABSE Conference, Guangzhou, China*, 8–11.

Fang, S.-E. and Perera, R. (2009). “A response surface methodology based damage identification technique.” *Smart Materials and Structures*, 18(6), 065009.

Fang, S.-E. and Perera, R. (2011). “Damage identification by response surface based model updating using d-optimal design.” *Mechanical Systems and Signal Processing*, 25(2), 717–733.

Feng, D., Scarangello, T., Feng, M. Q., and Ye, Q. (2017). “Cable tension force estimate using novel noncontact vision-based sensor.” *Measurement*, 99, 44–52.

Feng, Y., Lan, C., Briseghella, B., Fenu, L., and Zordan, T. (2022). “Cable optimization of a cable-stayed bridge based on genetic algorithms and the influence matrix method.” *Engineering Optimization*, 54(1), 20–39.

Ferreira, F. L. and Simoes, L. M. (2011). "Optimum design of a controlled cable stayed bridge subject to earthquakes." *Structural and Multidisciplinary Optimization*, 44(4), 517–528.

Friswell, M. and Mottershead, J. E. (1995). *Finite element model updating in structural dynamics*, Vol. 38. Springer Science & Business Media.

Gentile, C. and Cabboi, A. (2015). "Vibration-based structural health monitoring of stay cables by microwave remote sensing." *Smart Struct. Syst*, 16(2), 263–280.

Gentile, C. and Martinez Y Cabrera, F. (2004). "Dynamic performance of twin curved cable-stayed bridges." *Earthquake engineering & structural dynamics*, 33(1), 15–34.

Gentile, C. and Siviero, E. (2007). "Dynamic characteristics of the new curved cable-stayed bridge in porto marghera (venice, italy) from ambient vibration measurements." *IMAC-XXV*, 1–10.

Graff, K. F. (2012). *Wave motion in elastic solids*. Courier Corporation.

Haji Agha Mohammad Zarbaf, S. E., Norouzi, M., Allemang, R. J., Hunt, V. J., and Helmicki, A. (2017). "Stay cable tension estimation of cable-stayed bridges using genetic algorithm and particle swarm optimization." *Journal of Bridge Engineering*, 22(10), 05017008.

Halpern, A. B. and Billington, D. P. (2013). "Eminent structural engineer: Michel virlogeux–structural artist of modern french bridges." *Structural Engineering International*, 23(3), 350–353.

He, L., Castoro, C., Aloisio, A., Zhang, Z., Marano, G. C., Gregori, A., Deng, C., and Briseghella, B. (2022). "Dynamic assessment, fe modelling and parametric updating of a butterfly-arch stress-ribbon pedestrian bridge." *Structure and Infrastructure Engineering*, 18(7), 1064–1075.

Hofmeister, B., Bruns, M., and Rolfes, R. (2019). "Finite element model updating using deterministic optimisation: A global pattern search approach." *Engineering Structures*, 195, 373–381.

Horta, L. G., Reaves, M. C., Buehrle, R. D., Templeton, J. D., Lazor, D. R., Gaspar, J. L., Parks, R. A., and Bartolotta, P. A. (2011). "Finite element model calibration approach for ares ix." *Structural Dynamics, Volume 3*, Springer, 1037–1054.

Hua, X., Ni, Y., Chen, Z., and Ko, J. (2009). "Structural damage detection of cable-stayed bridges using changes in cable forces and model updating." *Journal of structural engineering*, 135(9), 1093–1106.

Irvine, H. (1981). “Cable structures the mit press.” *Cambridge, MA*, 15–24.

Jaishi, B. and Ren, W.-X. (2005). “Structural finite element model updating using ambient vibration test results.” *Journal of structural engineering*, 131(4), 617–628.

Jones, D. F., Mirrazavi, S. K., and Tamiz, M. (2002). “Multi-objective meta-heuristics: An overview of the current state-of-the-art.” *European journal of operational research*, 137(1), 1–9.

Kaczinski, M. et al. (2016). “Steel bridge design handbook: Bearing design.” *Report no.*, United States. Federal Highway Administration. Office of Bridges and Structures.

Kennedy, J. and Eberhart, R. (1995). “Particle swarm optimization.” *Proceedings of ICNN’95-International Conference on Neural Networks*, Vol. 4, IEEE, 1942–1948.

Kim, H. and Adeli, H. (2005). “Wavelet-hybrid feedback linear mean squared algorithm for robust control of cable-stayed bridges.” *Journal of Bridge Engineering*, 10(2), 116–123.

Kim, K.-S. and Lee, B.-I. (2012). “Current trends in concrete cable stayed bridge.” *Magazine of the Korea Concrete Institute*, 24(2), 10–15.

Li, H. and Ou, J. (2016). “The state of the art in structural health monitoring of cable-stayed bridges.” *Journal of Civil Structural Health Monitoring*, 6(1), 43–67.

Lin, K., Xu, Y.-L., Lu, X., Guan, Z., and Li, J. (2020a). “Cluster computing-aided model updating for a high-fidelity finite element model of a long-span cable-stayed bridge.” *Earthquake Engineering & Structural Dynamics*, 49(9), 904–923.

Lin, K., Xu, Y.-L., Lu, X., Guan, Z., and Li, J. (2020b). “Time history analysis-based nonlinear finite element model updating for a long-span cable-stayed bridge.” *Structural Health Monitoring*, 1475921720963868.

Lopez Aenlle, M., Brincker, R., and Fernandez Canteli, A. (2005). “Some methods to determine scaled mode shapes in natural input modal analysis.” *Proc. Int. Modal Analysis Conference (IMAC-XXIII)* cited By 15.

López Aenlle, M., Fernández Fernández, P., Brincker, R., Fernández Canteli, A. C., et al. (2007). “Scaling factor estimation using an optimized mass change strategy, part 1: theory.” *Proceedings* *of the 2nd international operational modal analysis conference*, Aalborg Universitet.

Martins, A. M., Simões, L. M., and Negrão, J. H. (2020). "Optimization of cable-stayed bridges: A literature survey." *Advances in Engineering Software*, 149, 102829.

Martí, R., Pardalos, P. M., and Resende, M. G. C. (2018). *Handbook of Heuristics*. Springer Publishing Company, Incorporated, 1st edition.

Mehrabi, A. B. and Tabatabai, H. (1998). "Unified finite difference formulation for free vibration of cables." *Journal of Structural Engineering*, 124(11), 1313–1322.

Miranda, L. J. V. (2018). "PySwarms, a research-toolkit for Particle Swarm Optimization in Python." *Journal of Open Source Software*, 3.

Nazarian, E., Ansari, F., Zhang, X., and Taylor, T. (2016). "Detection of tension loss in cables of cable-stayed bridges by distributed monitoring of bridge deck strains." *Journal of Structural Engineering*, 142(6), 04016018.

Ni, Y., Zhou, H., Chan, K., and Ko, J. (2008). "Modal flexibility analysis of cable-stayed ting kau bridge for damage identification." *Computer-Aided Civil and Infrastructure Engineering*, 23(3), 223–236.

Ni, Y.-C., Zhang, Q.-W., and Liu, J.-F. (2019). "Dynamic property evaluation of a long-span cable-stayed bridge (sutong bridge) by a bayesian method." *International Journal of Structural Stability and Dynamics*, 19(01), 1940010.

Park, W., Kim, H.-K., and Jongchil, P. (2012). "Finite element model updating for a cable-stayed bridge using manual tuning and sensitivity-based optimization." *Structural Engineering International*, 22(1), 14–19.

Park, W., Park, J., and Kim, H.-K. (2015). "Candidate model construction of a cable-stayed bridge using parameterised sensitivity-based finite element model updating." *Structure and Infrastructure Engineering*, 11(9), 1163–1177.

Parloo, E., Cauberghe, B., Benedettini, F., Alaggio, R., and Guillaume, P. (2005). "Sensitivity-based operational mode shape normalisation: Application to a bridge." *Mechanical Systems and Signal Processing*, 19(1), 43–55 cited By 73.

Parloo, E., Guillaume, P., Anthonis, J., Heylen, W., and Swevers, J. (2003). "Modelling of sprayer boom dynamics by means of maximum likelihood identification techniques, part 1: A comparison of input-output and output-only modal testing." *Biosystems Engineering*, 85(2), 163–171 cited By 21.

Parloo, E., Verboven, P., Cuillame, P., and Overmeire, M. (2001). "Sensitivity-based mass normalization of mode shape estimates from output-only data." *Proc. Int. Conf. on Structural System Identification*, 627–636 cited By 21.

Parloo, E., Verboven, P., Guillaume, P., and Van Overmeire, M. (2002). "Sensitivity-based operational mode shape normalisation." *Mechanical Systems and Signal Processing*, 16(5), 757–767 cited By 183.

Pasca, D. P., Aloisio, A., Fragiacomo, M., and Tomasi, R. (2021). "Dynamic characterization of timber floor subassemblies: Sensitivity analysis and modeling issues." *Journal of Structural Engineering*, 147(12), 05021008.

Petersen, Ø. W. and Øiseth, O. (2017). "Sensitivity-based finite element model updating of a pontoon bridge." *Engineering Structures*, 150, 573–584.

Petersen, Ø. W., Øiseth, O., Nord, T. S., and Lourens, E. (2018). "Estimation of the full-field dynamic response of a floating bridge using kalman-type filtering algorithms." *Mechanical Systems and Signal Processing*, 107, 12–28.

Pinqi, X. and Brownjohn, J. M. (2003). "Finite element modeling and model updating of a cable-stayed bridge." *Journal of Vibration Engineering*, 16(2), 219–223.

Rainieri, C. and Fabbrocino, G. (2014). "Operational modal analysis of civil engineering structures." *Springer, New York*, 142, 143.

Saisana, M., Saltelli, A., and Tarantola, S. (2005). "Uncertainty and sensitivity analysis techniques as tools for the quality assessment of composite indicators." *Journal of the Royal Statistical Society: Series A (Statistics in Society)*, 168(2), 307–323.

Saltelli, A. and Sobol', I. M. (1995). "Sensitivity analysis for nonlinear mathematical models: numerical experience." *Matematicheskoe Modelirovanie*, 7(11), 16–28.

Schlune, H., Plos, M., and Gylltoft, K. (2009). "Improved bridge evaluation through finite element model updating using static and dynamic measurements." *Engineering structures*, 31(7), 1477–1485.

Sehgal, S. and Kumar, H. (2016). "Structural dynamic model updating techniques: A state of the art review." *Archives of Computational Methods in Engineering*, 23(3), 515–533.

Shahverdi, H., Mares, C., and Mottershead, J. (2005). "Model structure correction and updating of aeroengine casings using fictitious mass modifications." *Proceedings of the Institution of Mechanical Engineers, Part C: Journal of Mechanical Engineering Science*, 219(1), 19–30 cited By 12.

Sheibani, M. and Ghorbani-Tanha, A. (2021). "Obtaining mass normalized mode shapes of motorway bridges based on the effect of traffic movement." *Structures*, Vol. 33, Elsevier, 2253–2263.

Simoen, E., De Roeck, G., and Lombaert, G. (2015). "Dealing with uncertainty in model updating for damage assessment: A review." *Mechanical Systems and Signal Processing*, 56, 123–149.

Siringoringo, D. M. and Fujino, Y. (2007). "Dynamic characteristics of a curved cable-stayed bridge identified from strong motion records." *Engineering Structures*, 29(8), 2001–2017.

Sobol', I. M. (1990). "On sensitivity estimation for nonlinear mathematical models." *Matematicheskoe modelirovanie*, 2(1), 112–118.

Song, W.-K., Kim, S.-E., and Ma, S. S. (2007). "Nonlinear analysis of steel cable-stayed bridges." *Computer-Aided Civil and Infrastructure Engineering*, 22(5), 358–366.

Storn, R. and Price, K. (1997). "Differential evolution–a simple and efficient heuristic for global optimization over continuous spaces." *Journal of global optimization*, 11(4), 341–359.

Talebinejad, I., Fischer, C., and Ansari, F. (2011). "Numerical evaluation of vibration-based methods for damage assessment of cable-stayed bridges." *Computer-Aided Civil and Infrastructure Engineering*, 26(3), 239–251.

Tian, Y., Wang, L., and Zhang, J. (2021). "Time-varying frequency-based scaled flexibility identification of a posttensioned concrete bridge through vehicle–bridge interaction analysis." *Structural Control and Health Monitoring*, 28(1), e2631.

Tian, Y., Zhang, J., and Han, Y. (2019). "Structural scaling factor identification from output-only data by a moving mass technique." *Mechanical Systems and Signal Processing*, 115, 45–59.

Virlogeux, M. (1999). "Recent evolution of cable-stayed bridges." *Engineering structures*, 21(8), 737–755.

Wen, Q., Hua, X., Chen, Z., Yang, Y., and Niu, H. (2016). "Control of human-induced vibrations of a curved cable-stayed bridge: design, implementation, and field validation." *Journal of Bridge Engineering*, 21(7), 04016028.

Wilson, J. C. and Liu, T. (1991). "Ambient vibration measurements on a cable-stayed bridge." *Earthquake engineering & structural dynamics*, 20(8), 723–747.

Wolpert, D. and Macready, W. (1997). "No free lunch theorems for optimization." *IEEE Transactions on Evolutionary Computation*, 1(1), 67–82.

Xiao, X., Xu, Y. L., and Zhu, Q. (2015). "Multiscale modeling and model updating of a cable-stayed bridge. ii: Model updating using modal frequencies and influence lines." *Journal of Bridge Engineering*, 20(10), 04014113.

Yang, D.-H., Yi, T.-H., Li, H.-N., and Zhang, Y.-F. (2018). "Monitoring and analysis of thermal effect on tower displacement in cable-stayed bridge." *Measurement*, 115, 249–257.

Zárate, B. A. and Caicedo, J. M. (2008). "Finite element model updating: Multiple alternatives." *Engineering Structures*, 30(12), 3724–3730.

Zhang, E., Shan, D., Guo, S., Ren, J., and Li, Q. (2017). "Influence of curvature radius on static and dynamic characteristics of curved cable-stayed bridge." *IABSE Symposium: Engineering the Future, Vancouver, Canada, 21-23 September 2017*, 793–800.

Zhang, Q., Chang, T.-Y. P., and Chang, C. C. (2001). "Finite-element model updating for the kap shui mun cable-stayed bridge." *Journal of Bridge Engineering*, 6(4), 285–293.

Zhang, Y. N. and Xie, J. (2019). "Compressive behaviour of laminated neoprene bridge bearing pads under thermal aging condition." *Materials Science Forum*, Vol. 972, Trans Tech Publ, 118–122.

Zhao, W., Zhang, G., and Zhang, J. (2020). "Cable force estimation of a long-span cable-stayed bridge with microwave interferometric radar." *Computer-Aided Civil and Infrastructure Engineering*, 35(12), 1419–1433.

Zhu, Q., Xu, Y. L., and Xiao, X. (2015). "Multiscale modeling and model updating of a cable-stayed bridge. i: Modeling and influence line analysis." *Journal of Bridge Engineering*, 20(10), 04014112.

Zhu, R., Li, F., Zhang, D., and Tao, J. (2019). "Effect of joint stiffness on deformation of a novel hybrid frp–aluminum space truss system." *Journal of Structural Engineering*, 145(11), 04019123.

List of Tables

TABLE 1. Comparison between the modal parameters estimated from experimental campaigns in 2010 and 2011.

No	f_{2010}[Hz]	f_{2011}[Hz]	$\frac{f_{2010}-f_{2011}}{f_{2010}}$ [%]	$\mathrm{MAC}_{2010-2011}$
1	0.635	0.635	0.00	0.988
2	0.996	0.996	0.00	0.980
3	1.143	1.143	0.00	0.958
4	1.387	1.387	0.00	0.998
5	1.523	1.523	0.00	0.982
6	1.602	1.602	0.00	0.990
7	1.953	1.963	-0.51	0.988
8	2.637	2.646	-0.34	0.983
9	3.174	/	/	/
10	4.053	4.072	-0.47	0.954
11	4.932	4.951	-0.39	0.836
12	5.596	5.625	-0.52	0.835

TABLE 2. Fundamental natural frequencies in [Hz] of the stay cables estimated in 2010 and 2011. The first nine values refer to the Mestre side, the second nine to the Venice side.

Stay cable no.	2010	2011
1	1.250	1.230
2	1.211	1.211
3	1.621	1.621
4	1.543	1.543
5	1.387	1.387
6	1.289	1.289
7	1.250	1.250
8	1.113	1.094
9	0.977	0.977
1	1.445	1.406
2	1.309	1.289
3	1.641	1.641
4	1.563	1.563
5	1.426	1.406
6	1.328	1.328
7	1.230	1.230
8	1.094	1.113
9	0.938	0.938

TABLE 3. Cable forces identified from vibration data in the tests of June 2010 and April 2011 (Mestre side)

	Mestre side, stay cable n.								
Cable force	1	2	3	4	5	6	7	8	9
T_{2010} [kN]	455	755	2350	3721	3866	4190	4825	5294	4746
T_{2011} [kN]	458	757	2359	3715	3842	4199	4828	5289	4771

TABLE 4. Cable forces identified from vibration data in the tests of June 2010 and April 2011 (Venice side)

Venice side, Stay cable n.									
Cable force	1	2	3	4	5	6	7	8	9
T_{2010} [kN]	647	906	2414	3771	4005	4324	4588	5275	4512
T_{2011} [kN]	614	860	2381	3704	3961	4352	4698	5310	4655

TABLE 5. Experimental numerical estimates of the cable forces before calibration.

Cable	Exp. [kN]	Num. [kN]	Error
M1	458	221	51.7%
M2	757	1342	-77.3%
M3	2359	2411	-2.2%
M4	3715	3516	5.4%
M5	3842	3384	11.9%
M6	4199	2961	29.5%
M7	4828	2513	47.9%
M8	5289	2311	56.3%
M9	4771	1986	58.4%
V1	614	353	42.5%
V2	860	1596	-85.6%
V3	2381	2844	-19.5%
V4	3704	4084	-10.3%
V5	3961	3979	-0.5%
V6	4352	3578	17.8%
V7	4698	2821	40.0%
V8	5310	2309	56.5%
V9	4655	1139	75.5%

TABLE 6. Comparison between experimental and numerical modal parameters before model updating, where f_e and f_n are the experimental and numerical natural frequencies.

No	Mode	f_e [Hz]	f_n [Hz]	$(f_e - f_n)/f_e$ [%]	MAC
1	V1	0.63	0.68	-6.49%	0.97
2	V2	1.00	0.97	2.12%	0.93
3	V3	1.14	1.23	-7.34%	0.86
4	T1	1.39	1.39	-0.54%	0.95
5	M1	1.52	1.65	-8.06%	0.80
6	T2	1.60	1.51	5.69%	0.76
7	V4	1.96	2.07	-5.49%	0.97
8	T3	2.65	2.56	3.31%	0.94
9	T5	4.07	3.99	1.91%	0.89
10	T6	4.95	4.84	2.17%	0.92
11	T7	5.63	5.54	1.53%	0.94

TABLE 7. Mass participation ratios of the modes before model updating. X, Y and Z indicate the longitudinal, transverse and vertical directions. U and R indicate the displacement and the rotation wth respect to the mentioned directions X, Y and Z.

Mode		Mass participation ratios [%]					
No	Label	Ux	Uy	Uz	Rx	Ry	Rz
1	V1	3.07	0.19	1.25	2.80	**14.00**	0.00
2	V2	1.29	**8.29**	**6.33**	**9.86**	0.02	0.43
3	V3	0.78	0.25	**11.14**	0.76	0.62	0.59
4	T1	2.85	**16.58**	0.35	0.16	0.01	0.28
5	M1	**9.56**	2.98	0.07	0.03	0.01	**17.40**
6	T2	0.95	**3.79**	1.34	0.10	0.04	**3.46**
7	V4	0.38	0.00	0.70	0.31	0.14	0.29
8	T3	0.01	0.00	0.00	0.06	0.08	0.00
9	T5	0.00	0.04	0.25	0.32	0.33	0.00
10	T6	0.00	0.00	0.04	1.78	**3.19**	0.00
11	T7	0.00	0.00	0.13	0.04	0.00	0.00

TABLE 8. Sensitivity indicators of the objective function in Eq.(3) to the Young's modulus of the tower (E_c), the mass of the steel deck (M_s), the mass of the concrete deck (M_c), the Young's modulus of the deck ($E_{c,deck}$), and the vertical stiffness of the bearings (k_a).

$E_{c,t}$	ρ_s	ρ_c	$E_{c,d}$	k_a
5.14%	0.34%	4.13%	1.21%	93.14%

TABLE 9. Sensitivity indicators of the cable forces labelled M1-M9 (Cables on the Mestre side) and V1-V9 (Cables on the Venice side) to the Young's modulus of the tower (E_c), the mass of the steel deck (M_s), the mass of the concrete deck (M_c), the Young's modulus of the deck ($E_{c,deck}$), and the vertical stiffness of the bearings (k_a)..

Cable force	$E_{c,t}$	ρ_s	ρ_c	$E_{c,d}$	k_a
M1	87.13%	0.08%	12.57%	0.51%	0.48%
M2	38.14%	0.25%	61.29%	1.37%	0.69%
M3	9.06%	0.27%	86.05%	1.35%	4.79%
M4	1.32%	0.23%	78.93%	1.12%	19.18%
M5	0.01%	0.17%	55.23%	0.79%	43.59%
M6	0.27%	0.12%	31.74%	0.47%	66.41%
M7	0.97%	0.07%	16.75%	0.24%	80.52%
M8	2.10%	0.05%	9.23%	0.11%	86.86%
M9	4.22%	0.03%	6.82%	0.07%	87.17%
V1	82.85%	0.18%	17.14%	0.22%	0.19%
V2	30.49%	0.39%	68.93%	0.95%	0.83%
V3	6.76%	0.41%	93.46%	1.32%	0.01%
V4	1.18%	0.36%	94.99%	1.44%	3.79%
V5	0.12%	0.29%	78.15%	1.28%	21.13%
V6	0.00%	0.20%	48.68%	0.91%	50.04%
V7	0.08%	0.12%	22.88%	0.48%	75.34%
V8	0.21%	0.05%	8.28%	0.15%	89.66%
V9	0.44%	0.01%	2.06%	0.02%	95.70%

TABLE 10. Sensitivity indicators of the objective function (OF) in Eq.(6) to the Young's modulus of the tower ($E_{c,t}$), the mass of the steel deck (ρ_s), the mass of the concrete deck (ρ_c), the Young's modulus of the deck ($E_{c,d}$), and the vertical stiffness of the bearings (k_a).

OF	$E_{c,t}$	$E_{c,d}$	ρ_c	ρ_s	k_a
$f(\boldsymbol{x})$	0.3%	0.5%	3.7%	0.0%	94.6%
$f_1(\boldsymbol{x})$	0.6%	0.9%	61.4%	0.1%	41.6%
$f_2(\boldsymbol{x})$	0.4%	0.7%	1.3%	0.0%	97.2%

TABLE 11. Sensitivity indicators of each natural frequency to the Young's modulus of the tower ($E_{c,t}$), the mass of the steel deck (ρ_s), the mass of the concrete deck (ρ_c), the Young's modulus of the deck ($E_{c,d}$), and the vertical stiffness of the bearings (k_a).

Mode	$E_{c,t}$	$E_{c,d}$	ρ_c	ρ_s	k_a
1-V1	3.2%	0.3%	42.2%	0.1%	54.6%
2-V2	94.4%	0.0%	4.4%	0.0%	4.4%
3-V3	17.0%	5.3%	75.4%	0.6%	23.3%
4-T1	3.8%	17.8%	52.9%	0.7%	39.2%
5-M1	0.1%	0.7%	48.9%	0.1%	53.2%
6-T2	0.0%	1.2%	65.4%	0.1%	33.8%
7-V4	0.0%	0.5%	49.3%	0.1%	51.0%
8-T3	1.4%	3.9%	65.8%	0.1%	34.1%
9-T5	0.0%	5.3%	60.2%	0.6%	52.3%
10-T6	1.9%	4.3%	54.8%	0.0%	48.3%
11-T7	0.0%	2.0%	52.0%	0.8%	51.9%

TABLE 12. Sensitivity indicators of the MAC of each mode to the Young's modulus of the tower ($E_{c,t}$), the mass of the steel deck (ρ_s), the mass of the concrete deck (ρ_c), the Young's modulus of the deck ($E_{c,d}$), and the vertical stiffness of the bearings (k_a).

Mode	$E_{c,t}$	$E_{c,d}$	ρ_c	ρ_s	k_a
1-V1	2.8%	2.6%	2.2%	0.0%	95.7%
2-V2	49.6%	0.2%	25.4%	0.0%	74.1%
3-V3	41.5%	16.3%	57.7%	0.2%	30.2%
4-T1	24.3%	58.3%	41.6%	0.4%	36.3%
5-M1	1.4%	3.8%	11.6%	0.0%	97.9%
6-T2	1.6%	48.8%	24.2%	0.1%	87.2%
7-V4	0.0%	0.0%	0.4%	0.0%	99.6%
8-T3	1.6%	0.6%	4.8%	0.2%	98.5%
9-T5	0.0%	0.9%	1.6%	0.0%	99.4%
10-T6	0.6%	0.6%	0.7%	0.0%	98.4%
11-T7	0.0%	0.6%	1.7%	0.0%	96.9%

TABLE 13. Cable forces and modal parameters associated with the optimum set of parameters and percentage error before and after the updating.

Cable Label	Exp. [kN]	Num. [kN]	Error	Initial error	Mode Label	Freq. Exp. [Hz]	Freq. Num. [Hz]	MAC	Freq. error	Initial MAC	Initial freq. error
M1	458	408	11%	52%	V1	0.635	0.699	97.10%	-10.1%	97.41%	-6.5%
M2	757	1228	-62%	-77%	V2	0.996	0.975	93.79%	2.1%	93.06%	2.1%
M3	2359	2372	-1%	-2%	V3	1.143	1.226	82.41%	-7.3%	85.58%	-7.3%
M4	3715	3852	-4%	5%	T1	1.387	1.395	95.03%	-0.6%	95.26%	-0.5%
M5	3842	4271	-11%	12%	M1	1.523	1.650	78.13%	-8.3%	80.01%	-8.1%
M6	4199	4453	-6%	29%	T2	1.602	1.513	75.38%	5.5%	75.56%	5.7%
M7	4828	4540	6%	48%	V4	1.963	2.073	97.04%	-5.6%	96.91%	-5.5%
M8	5289	5041	5%	56%	T3	2.646	2.559	94.04%	3.3%	94.19%	3.3%
M9	4771	4618	3%	58%	T5	4.072	3.995	89.03%	1.9%	89.10%	1.9%
V1	614	530	14%	43%	T6	4.951	4.826	93.29%	2.5%	91.61%	2.2%
V2	860	1279	-49%	-86%	T7	5.625	5.539	94.48%	1.5%	94.48%	1.5%
V3	2381	2460	-3%	-19%							
V4	3704	3872	-5%	-10%							
V5	3961	4284	-8%	0%							
V6	4352	4563	-5%	18%							
V7	4698	4573	3%	40%							
V8	5310	5229	2%	57%							
V9	4655	4791	-3%	76%							

TABLE 14. Optimized estimated modal parameters with their upper (U.B) and lower (L.B.) bounds.

Parameter	Unit	L.B.	U.B.	Optimum
ρ_c	kN/m^3	23	30	24
k_a	kN/mm	100	10000	1350
$E_{c,d}$	GPa	30	1	40
$E_{c,t}$	GPa	30	70	51.1

TABLE 15. Reaction forces on the Venice and Mestre side in case of rigid and flexible supports.

Label	Reaction [kN]		Relative difference	Displacement [mm]
	$k_a \to \infty$	$k_a = \hat{k}_a$		$k_a = \hat{k}_a$
Venice-1	9399.365	9302.627	1.03%	6.89
Venice-2	9055.16	8868.379	2.06%	6.57
Mestre-1	6705.512	6633.135	1.08%	4.91
Mestre-2	6480.927	6388.619	1.42%	4.73

List of Figures

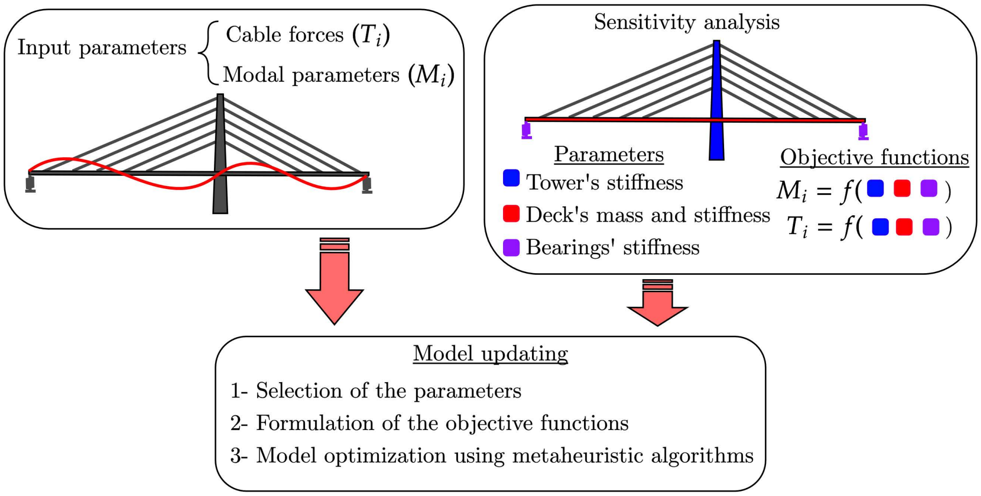

Fig. 1. Illustration of the followed procedure.

Fig. 2. View of the Porto Marghera Bridge (photographer: Bruno Briseghella).

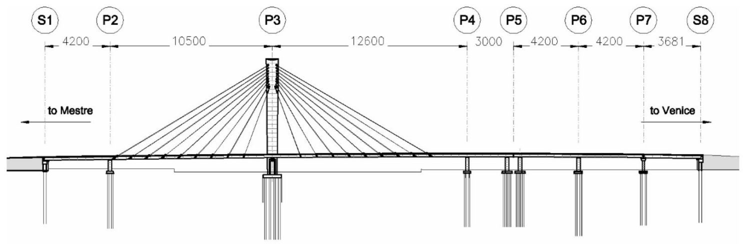

(a) Elevation.

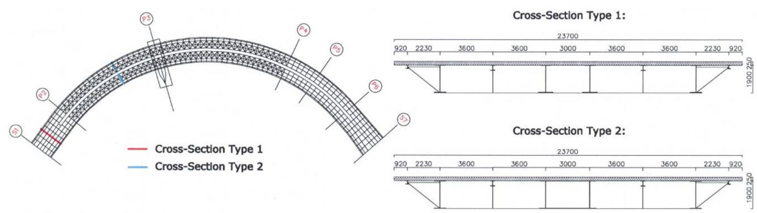

(b) Plan and typical cross sections.

Fig. 3. Schematic plan view of the deck and typical cross-sections (dimensions in cm in (a) and mm in (b)).

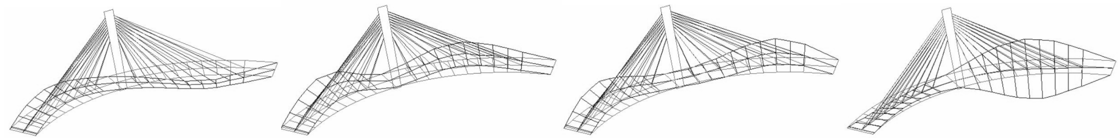

(a) $f_1 = \{0.635, 0.635\}$ **(b)** $f_2 = \{0.996, 0.996\}$ **(c)** $f_3 = \{1.143, 1.143\}$ **(d)** $f_4 = \{1.387, 1.387\}$

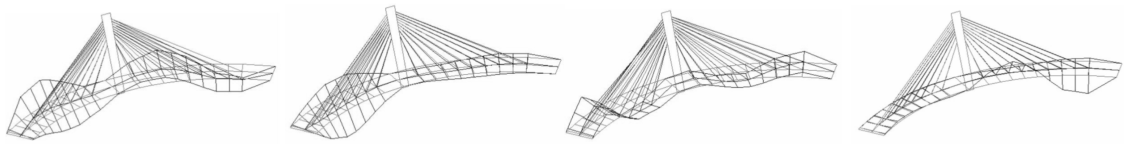

(e) $f_5 = \{1.523, 1.523\}$ **(f)** $f_6 = \{1.602, 1.602\}$ **(g)** $f_7 = \{1.193, 1.963\}$ **(h)** $f_8 = \{2.637, 2.646\}$

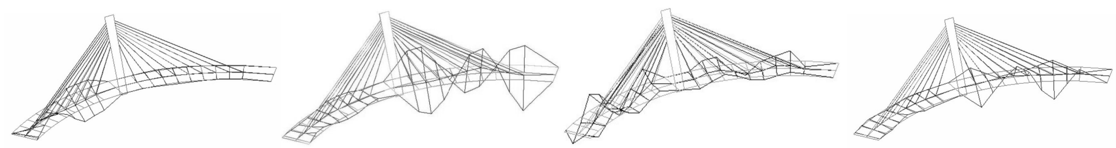

(i) $f_9 = \{3.174, /\}$ **(j)** $f_{10} = \{4.053, 4.072\}$ **(k)** f_{11} $\{4.932, 4.951\}$ = **(l)** $f_{12} = \{5.596, 5.625\}$

Fig. 4. Experimental mode shapes detected in the three experimental campaigns. The sub captions indicate the natural frequencies of each mode corresponding to the dynamic identifications carried out 2010 and 2011 respectively.

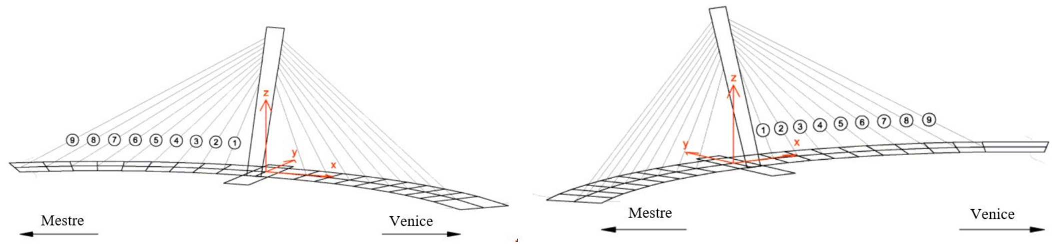

Fig. 5. Numbering of the stay cables.

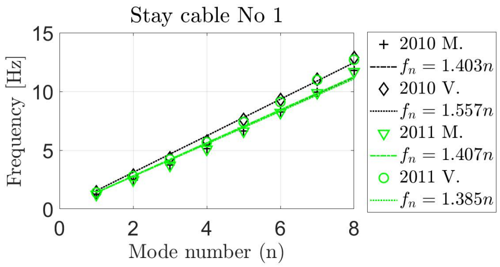

(a)

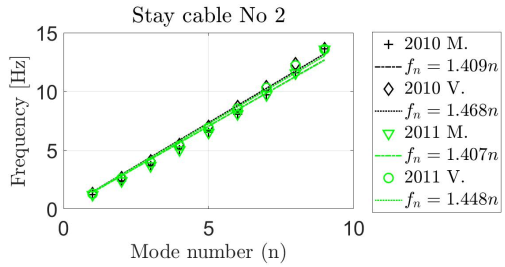

(b)

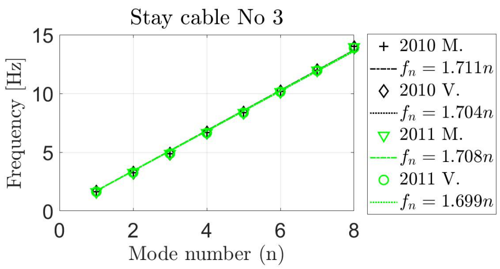

(c)

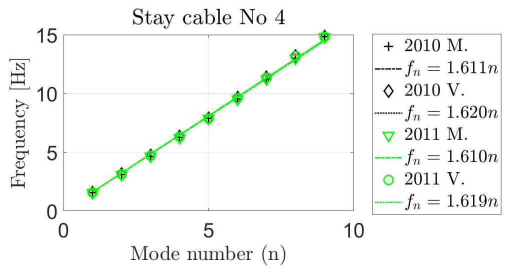

(d)

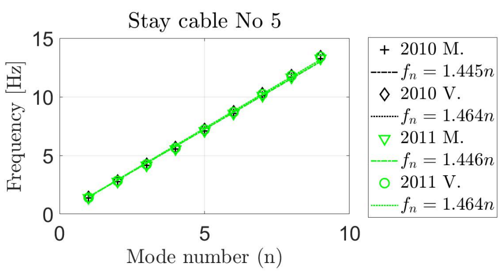

(e)

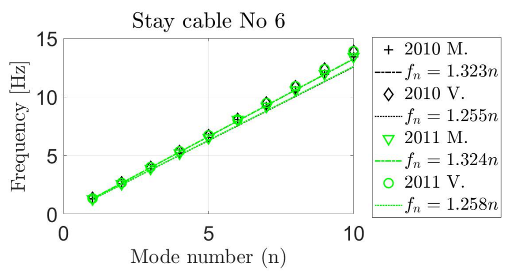

(f)

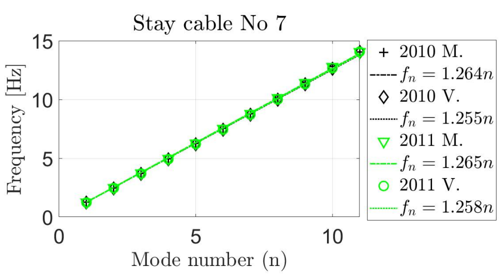

(g)

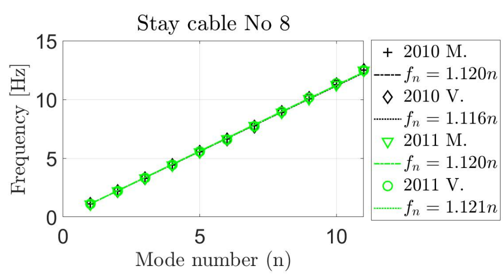

(h)

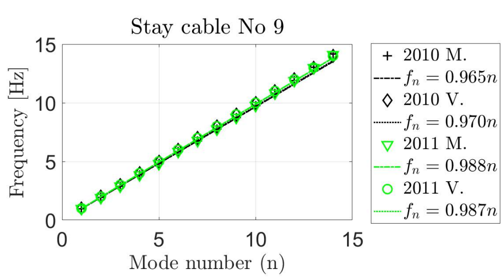

(i)

Fig. 6. Natural frequencies of the nine stay cables on the Mestre side and their correlation with the mode number.

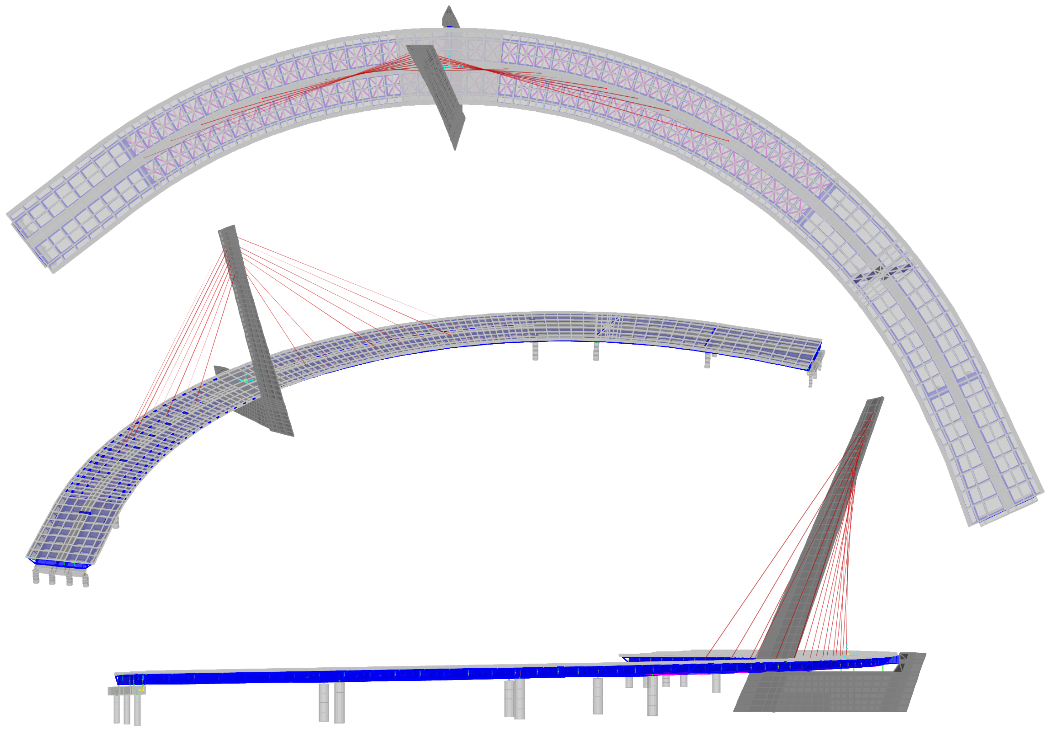

Fig. 7. FE model of the Porto Marghera bridge developed in SAP2000.

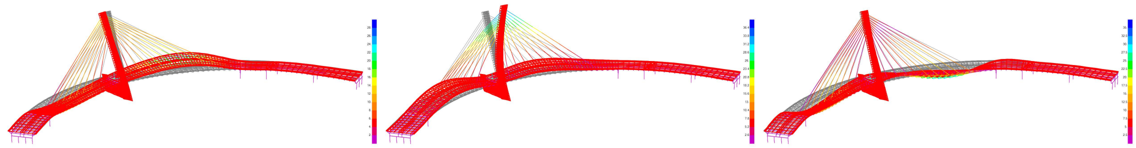

(a) f^e=0.635Hz; f^n=0.676Hz; MAC=0.97
(b) f^e=0.996Hz; f^n=0.975Hz; MAC=0.93
(c) f^e=1.143Hz; f^n=1.226Hz; MAC=0.85

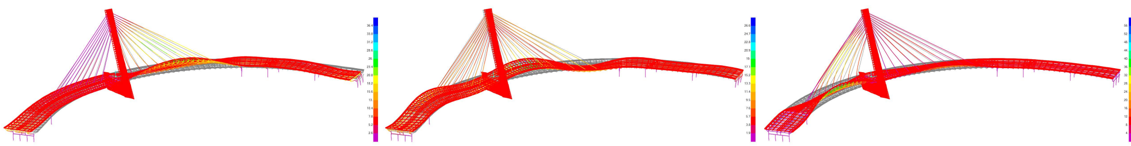

(d) f^e=1.387Hz; f^n=1.394Hz; MAC=0.95
(e) f^e=1.523Hz; f^n=1.646Hz; MAC=0.80
(f) f^e=1.602Hz; f^n=1.510Hz; MAC=0.75

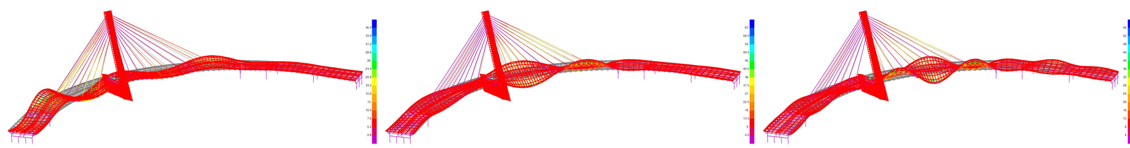

(g) f^e=1.963Hz; f^n=2.071Hz; MAC=0.96
(h) f^e=2.646Hz; f^n=2.559Hz; MAC=0.94
(i) f^e=4.072Hz; f^n=3.994Hz; MAC=0.89

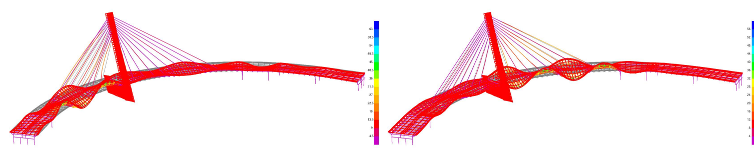

(j) f^e=4.951Hz; f^n=4.844Hz; MAC=0.91
(k) f^e=5.625Hz; f^n=5.539Hz; MAC=0.94

Fig. 8. Representation of a few selected numerical modes. f^e and f^n in the sub-captions indicate the experimental and numerical natural frequencies.

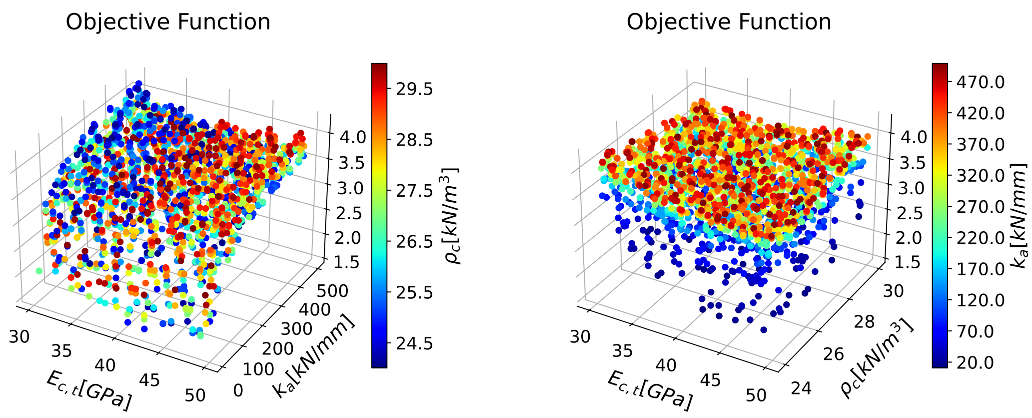

(a) **(b)**

Fig. 9. Different views of the scatter plot of the sensitivity of the objective function in Eq. (3) to the concrete Young's modulus of the tower (E_c, t), the vertical stiffness of the bearings (k_a) and the mass of the concrete deck (ρ_c).

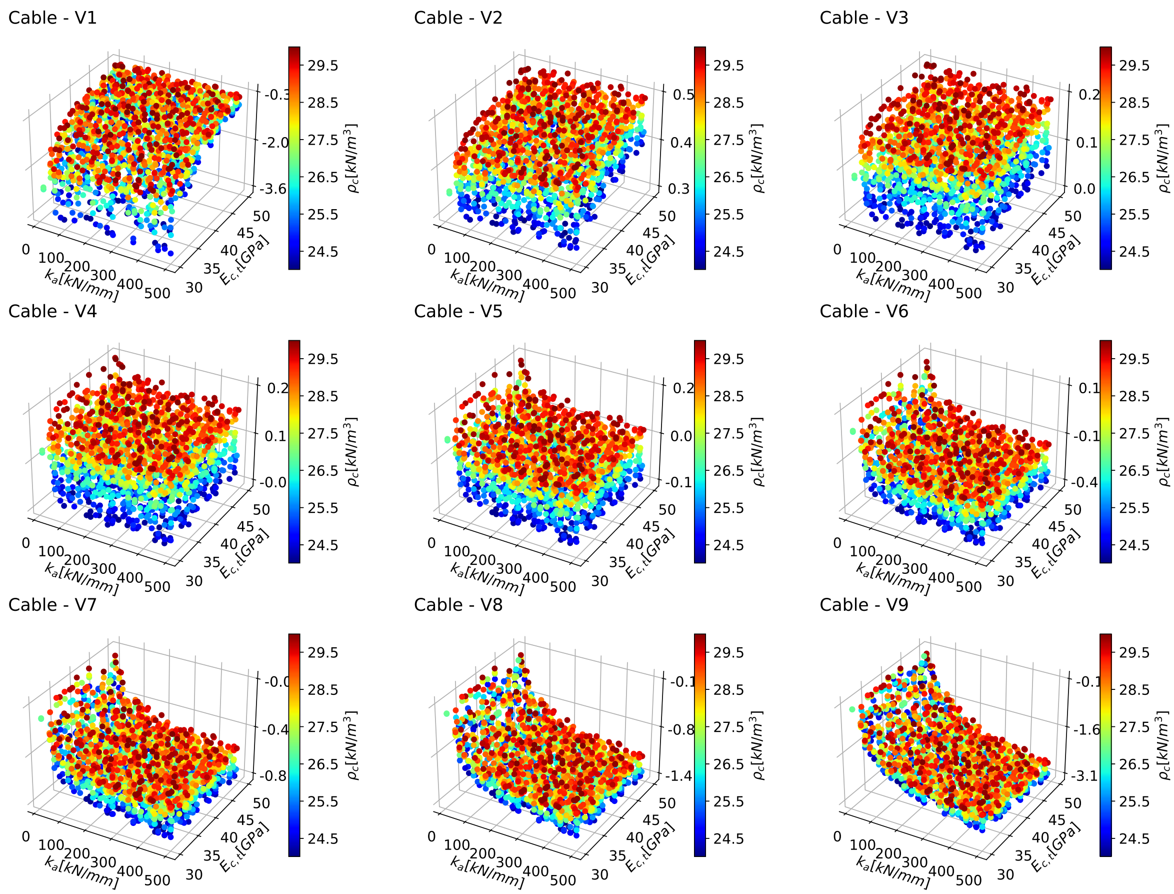

Fig. 10. Scatter plots of the sensitivity of the cable forces on the Venice side to the concrete Young's modulus of the tower ($E_{c,t}$), the vertical stiffness of the bearings (k_a) and the mass of the concrete deck (ρ_c).

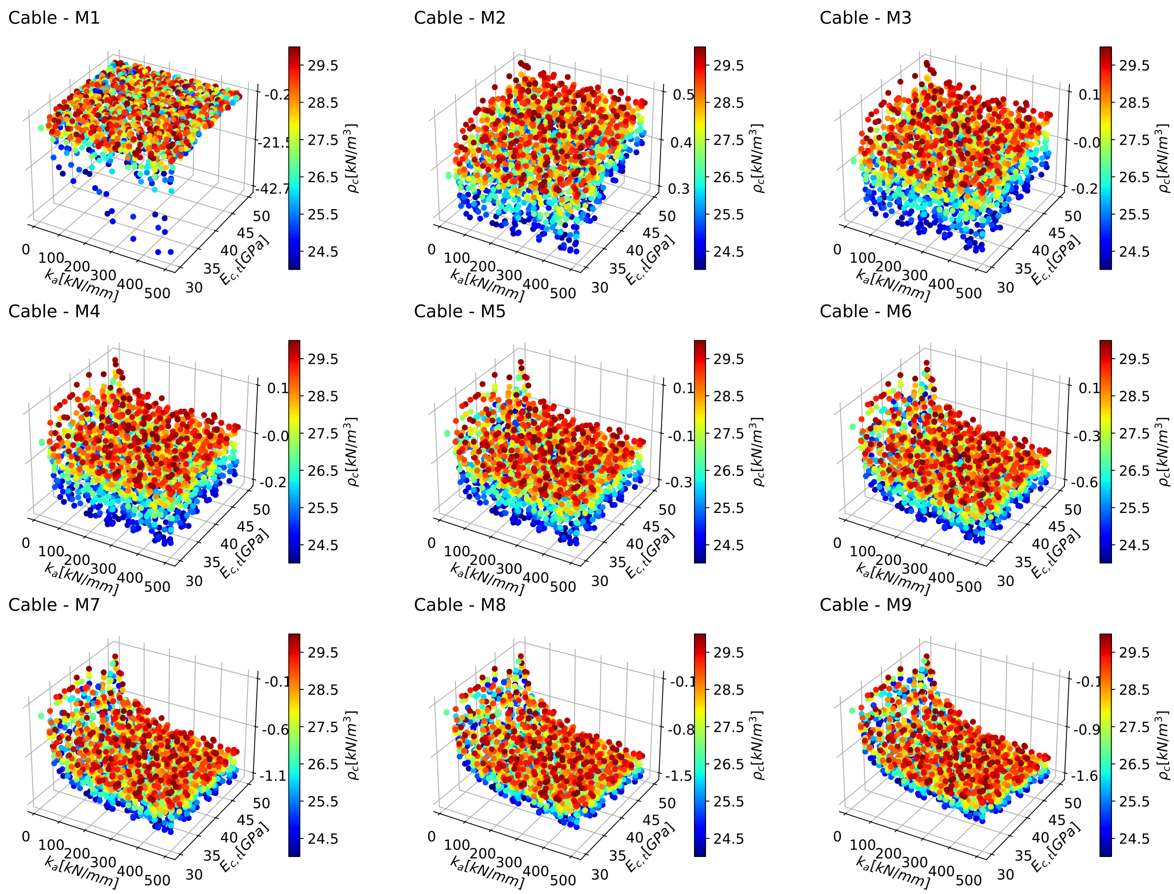

Fig. 11. Scatter plots of the sensitivity of the cable forces on the Mestre side to the concrete Young's modulus of the tower ($E_{c,t}$), the vertical stiffness of the bearings (k_a) and the mass of the concrete deck (ρ_c).

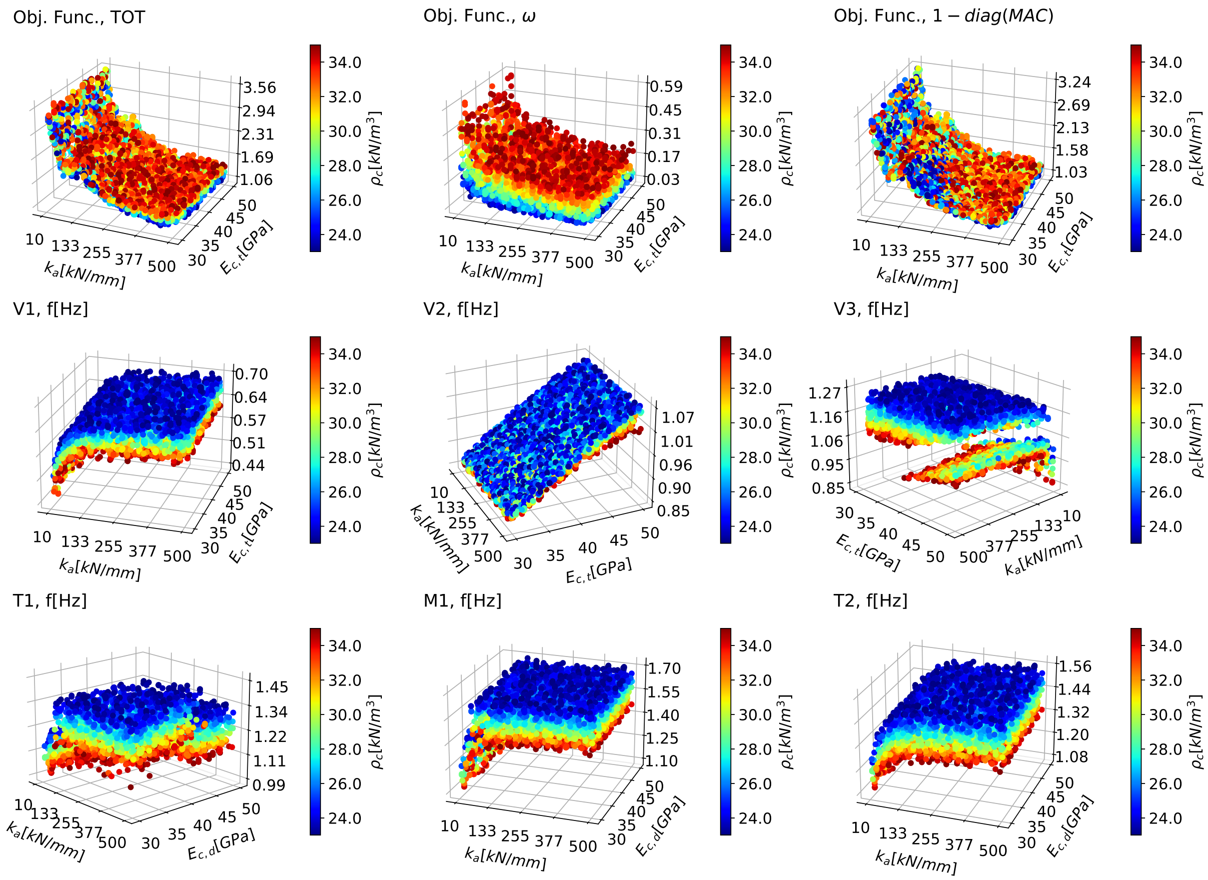

Fig. 12. Selected scatter plots of the sensitivity of the modal parameters to the concrete Young's modulus of the tower ($E_{c,t}$), the vertical stiffness of the bearings (k_a) and the mass of the concrete deck (ρ_c).

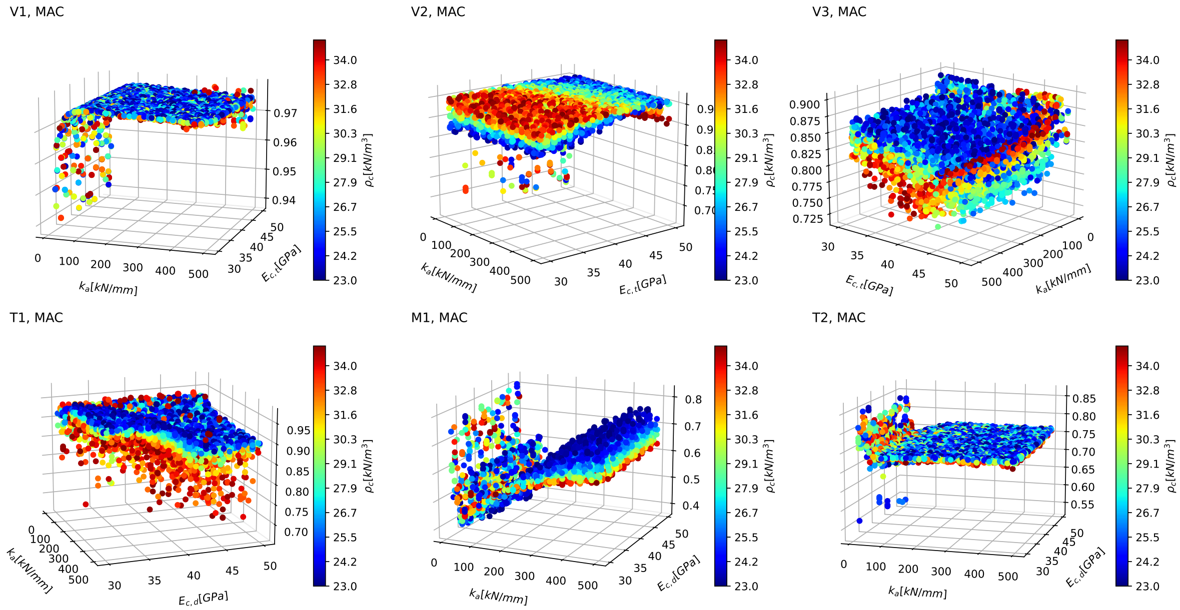

Fig. 13. Selected scatter plots of the sensitivity of the MAC to the concrete Young's modulus of the tower ($E_{c,t}$), the vertical stiffness of the bearings (k_a) and the mass of the concrete deck (ρ_c).